Chapter 4

A Relaxation Model for Coupled Two Spin $\frac{1}{2}$ Particles toward Thermal Equilibrium

A relaxation model of coupled two spin $\frac{1}{2}$ particles toward thermal equilibrium is presented. Raman-type dissipation mechanisms are introduced in addition to the usual bilinear coupling between the coupled system and the reservoir. The phase relaxation process and the energy relaxation process of the strongly coupled system are investigated.

4.1 Introduction

In the preceding chapters, we studied dynamics of the dissipative Jaynes-Cummings model using the relaxation model which describes dynamics toward the correct thermal equilibrium state of the coupled system. The relaxation model was derived from the microscopic point of view. We studied the relaxation dynamics by investigating the phase relaxation process and the energy relaxation process of the strongly coupled system. It is the very characteristic of our formulation that the elements of the reduced density matrix can be expanded in terms of the eigenstates (dressed states) of the strongly coupled system. We could microscopically unify dynamics of the different time domains; coherent motion of the coupled system, phase relaxation (decoherence), and energy relaxation processes.

In this chapter, we apply our formulation to another strongly coupled system, which consists of two spin $\frac{1}{2}$ particles interacting with each other strongly. Study of relaxation dynamics of coupled spin particles is not new. Indeed, the phenomenological relaxation model was proposed in 1950s [1] in connection with the nuclear spin relaxation [2]. But there was no study of the relaxation dynamics toward correct thermal equilibrium with fully quantum mechanical dissipative model. Recently, renewed attention is payed to this coupled system as the quantum gate of quantum computing [3], which requires to describe the system as the quantum mechanical dissipative model.

Significance of treating the coupled system as another prototype of the dissipative coupled system is that the eigenstates are exact whereas the Jaynes-Cummings model is solved within the rotating wave approximation. It is also a characteristic of the model that the density matrix is expanded in terms of finite number of elements, whereas the Jaynes-Cummings model has infinite number of elements originating from the character of boson operator.

4.2 System

4.2.1 The coupled system

Our system consists of two spin $\frac{1}{2}$ particles which are expressed by spin operators $\boldsymbol{S}_1 = (S_1^x,\ S_1^y,\ S_1^z)$ and $\boldsymbol{S}_2 = (S_2^x,\ S_2^y,\ S_2^z)$. The Hamiltonian of the coupled system is given by

$$H = H_0 + H_i \tag{4.2.1}$$

where

$$H_0 = \hbar\omega_1 S_1^z + \hbar\omega_2 S_2^z, \tag{4.2.2}$$

$$H_i = \frac{\hbar g}{2}\left(S_1^+ S_2^- + S_1^- S_2^+\right) + \hbar g_z S_1^z S_2^z \tag{4.2.3}$$

in which $S_\alpha^\pm \equiv S_\alpha^x \pm i S_\alpha^y$ for $\alpha = 1, 2$ and ω_1, ω_2 are Larmor frequencies. This Hamiltonian contains the anisotropic case ($g \neq g_z$) and case of interaction of two different kind of spin ($\omega_1 \neq \omega_2$), so it can describe general interactions of two spin $\frac{1}{2}$ particles.

The coupled system has four eigenstates which are expressed in terms of the product states of two spins:

$$|1\rangle \equiv |-\rangle_1 |-\rangle_2, \tag{4.2.4}$$

$$|2\rangle \equiv -\sin\theta\, |+\rangle_1 |-\rangle_2 + \cos\theta\, |-\rangle_1 |+\rangle_2, \tag{4.2.5}$$

$$|3\rangle \equiv \cos\theta\, |+\rangle_1 |-\rangle_2 + \sin\theta\, |-\rangle_1 |+\rangle_2, \tag{4.2.6}$$

$$|4\rangle \equiv |+\rangle_1 |+\rangle_2. \tag{4.2.7}$$

where we denote the spin up $(+)$ and down $(-)$ states of the particle α as $|\pm\rangle_\alpha$ and with

$$\tan\theta = \frac{g}{\Delta\omega + \lambda}, \tag{4.2.8}$$

$$\Delta\omega \equiv \omega_1 - \omega_2, \tag{4.2.9}$$

$$\lambda \equiv \sqrt{(\Delta\omega)^2 + g^2}. \tag{4.2.10}$$

The eigenstates are mutually orthogonal and satisfy the completeness condition. The corresponding energy eigenvalues E_n of $H|n\rangle = E_n|n\rangle$ are given as

$$E_1 = -\frac{\hbar}{2}(\omega_1 + \omega_2) + \frac{\hbar g_z}{4} \tag{4.2.11}$$

$$E_2 = -\frac{\hbar\lambda}{2} - \frac{\hbar g_z}{4} \tag{4.2.12}$$

$$E_3 = \frac{\hbar\lambda}{2} - \frac{\hbar g_z}{4} \tag{4.2.13}$$

$$E_4 = \frac{\hbar}{2}(\omega_1 + \omega_2) + \frac{\hbar g_z}{4}. \tag{4.2.14}$$

Since we do not use any approximation to derive the eigenstates, we are free to vary strength of the coupling constants g, g_z between the two particles.

4.2.2 Interaction between the coupled system and the reservoir

We want to describe effects of the environment which surrounds the coupled two spin $\frac{1}{2}$ particle system. The coupled system is assumed to interact weakly with a reservoir consisting of many mode bosons. The reservoir gives dissipative effects to the coupled system and leads the coupled system relaxing toward thermal equilibrium at a given temperature T. The Hamiltonian of the reservoir is given by

$$H_B = \hbar \sum_l \omega_l B_l^\dagger B_l \tag{4.2.15}$$

with $\omega_l > 0$, where $B_l^\dagger$ and B_l represent the creation and the annihilation operators of the reservoir bosons. We assume that the reservoir bosons always stay in the thermal equilibrium since the reservoir has large degrees of freedom than the coupled system. In short, the reservoir is in the canonical distribution at the given temperature T.

Next, we introduce the interaction of the coupled system with the reservoir. Usual bilinear interaction which causes energy exchange of each spin $\frac{1}{2}$ particle, i.e. interaction giving rise to an absorption-emission type dissipation mechanisms is given by

$$H_{\alpha B} = \hbar \left(S_\alpha^- + S_\alpha^+\right) g_{\alpha B} \sum_l \left(B_l^\dagger + B_l\right) \tag{4.2.16}$$

for $\alpha = 1, 2$. This is the first order interaction. We also introduce the second order interaction between the system and the reservoir which expresses the Raman type dissipation process as

$$H_{iB} = \hbar \left(S_1^+ S_2^\mp + S_1^- S_2^\pm\right) g_{iB} \sum_l \left(B_l^\dagger + B_l\right) \tag{4.2.17}$$

for $i = +, -$: $i = +$ corresponds to the upper superscript while $i = -$ to the lower.

It must be pointed out that we have to take into account the counter rotating part of the interaction between the system operators and the reservoir operators whereas in the conventional treatment, the rotating wave approximation is widely used, for instance, the interaction is given by

$$H_c = \hbar g_{\alpha B} \sum_l \left(S_\alpha^- B_l^\dagger + S_\alpha^+ B_l \right). \tag{4.2.18}$$

The requirement of taking the counter rotating part is due to the same reason of that as for the dissipative Jaynes-Cummings model, the counter rotating term is necessary when the coupling between the two spins becomes strong, $g \gg \omega_1, \omega_2$, where the energy level reversal $E_n > E_m$ for $n < m$ occurs.

4.3 Equations of motion

In this section, we start from the master equation which ensures the coupled system relaxing to the correct canonical distribution and we derive a set of solvable equations of motion using the eigenstates of the coupled system.

By the projection operator method (TCL formalism), we reduce the Liouville von Neumann equation of the whole system including the reservoir operators into the generalized master equation for the density operator of the coupled system only (reduced density operator). Owing to the condition that the coupling between the coupled system and the reservoir is weak, it is enough to take into account the terms up to the second order of the interaction between the coupled system and the reservoir. Thus, the resulting master equation is obtained as

$$\frac{\partial}{\partial t}\rho(t) = \frac{1}{i\hbar}[H\,,\rho(t)\,] + \sum_{\alpha=1,2}\Gamma_\alpha\,\rho(t) + \sum_{i=\pm}\Gamma_i\,\rho(t) \tag{4.3.1}$$

where

$$\begin{aligned}
\Gamma_\alpha\rho(t) &= \sum_l g_{\alpha B}^2\int_0^t dt'\Big\{\Big(\langle B_l^\dagger(t')\,B_l\rangle_B + \langle B_l(t')\,B_l^\dagger\rangle_B\Big) \\
&\times \Big(\big[S_\alpha^+(-t')\,\rho(t)\,,S_\alpha^-\big] + \big[S_\alpha^-(-t')\,\rho(t)\,,S_\alpha^+\big]\Big) \\
&+ \Big(\langle B_l^\dagger(-t')\,B_l\rangle_B + \langle B_l(-t')\,B_l^\dagger\rangle_B\Big) \\
&\times \Big(\big[S_\alpha^+,\ \rho(t)\,S_\alpha^-(-t')\big] + \big[S_\alpha^-,\ \rho(t)\,S_\alpha^+(-t')\big]\Big)\Big\}
\end{aligned} \tag{4.3.2}$$

and

$$\begin{aligned}
\sum_{i=\pm}\Gamma_i\rho(t) &= \sum_l g_{iB}^2\int_0^t dt'\Big\{\Big(\langle B_l^\dagger(t')\,B_l\rangle_B + \langle B_l(t')\,B_l^\dagger\rangle_B\Big) \\
&\times \Big(\big[\underline{S_1^+S_2^\mp}(-t')\,\rho(t)\,,S_1^-S_2^\pm\big] + \big[\underline{S_1^-S_2^\pm}(-t')\,\rho(t)\,,S_1^+S_2^\mp\big]\Big) \\
&+ \Big(\langle B_l^\dagger(-t')\,B_l\rangle_B + \langle B_l(-t')\,B_l^\dagger\rangle_B\Big) \\
&\times \Big(\big[S_1^+S_2^\mp,\rho(t)\,\underline{S_1^-S_2^\pm}(-t')\big] + \big[S_1^-S_2^\pm,\rho(t)\,\underline{S_1^+S_2^\mp}(-t')\big]\Big)\Big\}.
\end{aligned} \tag{4.3.3}$$

It is not necessary to take into account all the damping terms Γ_α and Γ_i at the same time but to select some of them for a physical situation under consideration.

In our formalism, we started from the Liouville von Neumann equation for the total system where the composite two spin system is interacting with the reservoir as a whole and then we reduced the reservoir operators to derive the master equation. In contrast, in the usual treatments which do not give the correct equilibrium distribution, the Liouville von Neumann equation for each subsystem interacting with a reservoir is reduced to obtain a master equation for each subsystem and then they are coupled mechanically. The characteristic point of the derived master equation by our method is that time evolution of the system operators in the damping terms are expressed by the full Hamiltonian of the coupled system: $S_\alpha^\pm(t) = \mathrm{e}^{iHt/\hbar} S_\alpha^\pm \mathrm{e}^{-iHt/\hbar}$ and $\underline{S_1^\pm S_2^\mp}(t) = \mathrm{e}^{iHt/\hbar} S_1^\pm S_2^\mp \mathrm{e}^{-iHt/\hbar}$. This ensures the coupled system evolving in time toward the correct thermal equilibrium, as in the same way for the dissipative Jaynes-Cummings model in the previous chapters.

Next, we expand all the operators in the master equation in terms of the eigenstates and derive equations of motion for the expansion coefficients of the reduced density operator

$$\rho_{nm}(t) \equiv \langle n| \rho(t) |m\rangle . \tag{4.3.4}$$

For instance, the following operators appearing in the master equation are expanded in terms of the eigenstates as

$$\begin{aligned} S_\alpha^+(t) &= f_\alpha^1 \mathrm{e}^{i\epsilon_{21}t/\hbar} |2\rangle\langle 1| + f_\alpha^2 \mathrm{e}^{i\epsilon_{31}t/\hbar} |3\rangle\langle 1| \\ &+ f_\alpha^3 \mathrm{e}^{i\epsilon_{42}t/\hbar} |4\rangle\langle 2| + f_\alpha^4 \mathrm{e}^{i\epsilon_{43}t/\hbar} |4\rangle\langle 3| \end{aligned} \tag{4.3.5}$$

and

$$\begin{aligned} S_\alpha^z(t) &= -|1\rangle\langle 1| + d_\alpha^1 |2\rangle\langle 2| + d_\alpha^2 \mathrm{e}^{-i\epsilon_{32}t/\hbar} |2\rangle\langle 3| \\ &+ d_\alpha^2 \mathrm{e}^{i\epsilon_{32}t/\hbar} |3\rangle\langle 2| - d_\alpha^1 |3\rangle\langle 3| + |4\rangle\langle 4| \end{aligned} \tag{4.3.6}$$

for $\alpha = 1, 2$ with the coefficients

$$f_1^1 = -f_1^4 = -\sin\theta, \tag{4.3.7}$$

$$f_1^2 = f_1^3 = \cos\theta, \tag{4.3.8}$$

$$f_2^1 = f_2^4 = \cos\theta, \tag{4.3.9}$$

$$f_2^2 = -f_2^3 = \sin\theta, \tag{4.3.10}$$

$$d_1^1 = -d_2^1 = -\cos 2\theta, \tag{4.3.11}$$

$$d_1^2 = -d_2^2 = -\sin 2\theta \tag{4.3.12}$$

and ϵ_{nm} represents energy difference between the two eigenstates, $E_n - E_m$.

Further, we assume the narrowing limit condition, that is, the assumption that the characteristic time scale of the reservoir motion is much shorter than that of the coupled system. Thus we let the upper bound time t of the integral in the damping terms (4.3.2) and (4.3.3) to infinity. The correlation functions of the reservoir operators in the damping terms are calculated to give the thermal photon number functions, $\hat{n}_1(X)$ and $\hat{n}_2(X)$ together with the integral of the time dependent part of the system operators. The thermal photon number functions are defined by

$$\hat{n}_1(X) \equiv (\exp[X/k_BT] - 1)^{-1} \equiv \hat{n}(X), \tag{4.3.13}$$

$$\hat{n}_2(X) \equiv -(\exp[-X/k_BT] - 1)^{-1} = \hat{n}(X) + 1, \tag{4.3.14}$$

for $X > 0$, and

$$\hat{n}_1(X) \equiv -(\exp[X/k_BT] - 1)^{-1} = \hat{n}(-X) + 1, \tag{4.3.15}$$

$$\hat{n}_2(X) \equiv (\exp[-X/k_BT] - 1)^{-1} = \hat{n}(-X), \tag{4.3.16}$$

for $X < 0$. When $X = 0$, we have

$$\hat{n}_1(X) \equiv 0, \tag{4.3.17}$$

$$\hat{n}_2(X) \equiv 0. \tag{4.3.18}$$

In these expressions, necessary energy differences ϵ_{nm} should be substituted for X. The functions are the same as the ones appeared in the previous chapters.

Thus we have a solvable equation of motion for each expansion coefficient ρ_{nm}.

Introducing vectors by

$$\boldsymbol{\rho}_A(t) \equiv \begin{pmatrix} \rho_{11}(t) \\ \rho_{22}(t) \\ \rho_{23}(t) \\ \rho_{32}(t) \\ \rho_{33}(t) \\ \rho_{44}(t) \end{pmatrix}, \tag{4.3.19}$$

$$\boldsymbol{\rho}_B(t) \equiv \begin{pmatrix} \rho_{12}(t) \\ \rho_{13}(t) \\ \rho_{24}(t) \\ \rho_{34}(t) \end{pmatrix}, \tag{4.3.20}$$

$$\boldsymbol{\rho}_C(t) \equiv \begin{pmatrix} \rho_{14}(t) \end{pmatrix}, \tag{4.3.21}$$

and noting the Hermite condition of the density matrix:

$$\boldsymbol{\rho}_{B'}(t) \equiv \begin{pmatrix} \rho_{21}(t) \\ \rho_{31}(t) \\ \rho_{42}(t) \\ \rho_{43}(t) \end{pmatrix} = \boldsymbol{\rho}_B{}^*(t), \tag{4.3.22}$$

$$\boldsymbol{\rho}_{C'}(t) \equiv \begin{pmatrix} \rho_{41}(t) \end{pmatrix} = \boldsymbol{\rho}_C{}^*(t), \tag{4.3.23}$$

we have equations of motion written in a form of the first order vector simultaneous differential equation:

$$\frac{\partial}{\partial t}\boldsymbol{\rho}_X(t) = \left(\frac{1}{i\hbar}\boldsymbol{L}^X + \sum_{\alpha=1,2}\kappa_\alpha \boldsymbol{Q}_\alpha^X + \sum_{i=\pm}\kappa_i \boldsymbol{Q}_i^X\right)\boldsymbol{\rho}_X(t) \tag{4.3.24}$$

for $X = A, B, B', C, C'$; κ_α, κ_i are the damping constants which are written in terms of the coupling strength between the system operator and the reservoir operator. The first term on the right hand side of (4.3.24) expresses the coherent motion due to the first term of the right hand side of (4.3.1) and the second and the third terms are the damping terms originating from the absorption-emission type dissipation mechanism

(4.2.16) and the Raman type dissipation mechanism (4.2.17), respectively. The explicit forms of the coefficient matrices are given in the Appendix.

It is a characteristic feature of the equations of motion that they are divided into several groups, denoted by $A, B(B')$ and $C(C')$. The dissipation mechanisms which are given by the damping terms (4.3.2) and (4.3.3) do not give rise to mixing coefficients which belong to the different groups. This is due to the representation of operators in terms of the eigenstates. Thus the expectation values of the system operators are related to the elements of the groups A, B and C. Generally, an expectation value of a system operator G is given by $\langle G \rangle = \mathrm{Tr}\rho G$. Explicitly, expectation values of our system operators are written as

$$\langle S_1^z \rangle = -\rho_{11} - \cos 2\theta \rho_{22} - 2\sin 2\theta \mathrm{Re}\left[\rho_{23}\right] + \cos 2\theta \rho_{33} + \rho_{44}, \tag{4.3.25}$$

$$\langle S_2^z \rangle = -\rho_{11} + \cos 2\theta \rho_{22} + 2\sin 2\theta \mathrm{Re}\left[\rho_{23}\right] - \cos 2\theta \rho_{33} + \rho_{44} \tag{4.3.26}$$

which belong to the group A, and

$$\left\langle S_1^+ \right\rangle = -\sin\theta \rho_{12} + \cos\theta \rho_{13} + \cos\theta \rho_{24} + \sin\theta \rho_{34}, \tag{4.3.27}$$

$$\left\langle S_2^+ \right\rangle = +\cos\theta \rho_{12} + \sin\theta \rho_{13} - \sin\theta \rho_{24} + \cos\theta \rho_{34} \tag{4.3.28}$$

which belong to group B.

4.4 Calculation of dynamics

4.4.1 Initial condition

We choose the following initial condition on our spin $\frac{1}{2}$ particle system: Since our interest is to find how the effects of reservoir on the quantum state appear to destroy quantum coherence, we impose a pure state initial condition instead of the statistical mixture of the states. An arbitrary quantum state of the spin α particle is expressed by Bloch state as $|\theta_\alpha, \varphi_\alpha\rangle_\alpha$ for $\alpha = 1, 2$. We assume that the two spin $\frac{1}{2}$ particles begin to interact each other at $t = 0$ and also with the reservoir at the same time. Thus the coupled system is considered to be in the product state of these Bloch states at $t = 0$. That is, the initial condition for the density operator is written as

$$\rho(0) = |\theta_1, \varphi_1\rangle_1 \, {}_1\langle\theta_1, \varphi_1| \otimes |\theta_2, \varphi_2\rangle_2 \, {}_2\langle\theta_2, \varphi_2| \,. \tag{4.4.1}$$

Expanding the density operator $\rho(0)$ in terms of the eigenstates, the initial condition of the coefficient $\rho_{nm}(0)$ is calculated to be

$$\rho_{nm}(0) = G_n G_m^* \tag{4.4.2}$$

where

$$G_1 = \mathrm{e}^{-\frac{i}{2}(\varphi_1+\varphi_2)} \sin\frac{\theta_1}{2} \sin\frac{\theta_2}{2} \tag{4.4.3}$$

$$G_2 = \mathrm{e}^{-\frac{i}{2}(\varphi_1-\varphi_2)} \sin\frac{\theta_1}{2} \cos\frac{\theta_2}{2} \cos\theta - \mathrm{e}^{\frac{i}{2}(\varphi_1-\varphi_2)} \cos\frac{\theta_1}{2} \sin\frac{\theta_2}{2} \sin\theta \tag{4.4.4}$$

$$G_3 = \mathrm{e}^{-\frac{i}{2}(\varphi_1-\varphi_2)} \sin\frac{\theta_1}{2} \cos\frac{\theta_2}{2} \sin\theta + \mathrm{e}^{\frac{i}{2}(\varphi_1-\varphi_2)} \cos\frac{\theta_1}{2} \sin\frac{\theta_2}{2} \cos\theta \tag{4.4.5}$$

$$G_4 = \mathrm{e}^{\frac{i}{2}(\varphi_1+\varphi_2)} \cos\frac{\theta_1}{2} \cos\frac{\theta_2}{2}. \tag{4.4.6}$$

4.4.2 Numerical calculations

We solve the equation of motion (4.3.24) for groups A, B and C numerically by Runge Kutta method. In this thesis, we calculate the relaxation process with the absorption-

emission type dissipation mechanism and take $\kappa_\pm = 0$. We investigate relaxation dynamics of the strongly coupled system due to the dissipation mechanism from off-equilibrium initial conditions of $\theta_1 = \pi/4$, $\varphi_1 = \pi/2$, $\theta_2 = 5\pi/6$, $\varphi_1 = 5\pi/6$ toward the correct thermal equilibrium at temperature T:

$$\rho(\infty) = \frac{\sum_n e^{-E_n/k_B T} |n\rangle \langle n|}{\sum_n e^{-E_n/k_B T}}. \tag{4.4.7}$$

Calculation of expectation values

First, we show time evolution of expectation values. We calculated expectation values for longitudinal components of spins $\langle S_\alpha^z \rangle$ and the transverse components of spins $\langle S_\alpha^x \rangle = \mathrm{Re}\left[\langle S_\alpha^+ \rangle\right]$ and $\langle S_\alpha^y \rangle = \mathrm{Im}\left[\langle S_\alpha^+ \rangle\right]$ for spin $\alpha = 1$ and $\alpha = 2$ for various conditions. Relaxation of transverse components shows the phase relaxation and that of longitudinal components show the energy relaxation for each subsystem, spin 1 and spin 2.

In Fig.4.1, we show time evolution of expectation values with parameters $\kappa_1/g = \kappa_2/g = 0.01$, $g_z/g = 0$, $\omega_1/g = \omega_2/g = 2$, $T/g = 0.01$. With this condition, energy eigenvalues are given by $E_1 = -200.0$, $E_2 = -50.0$, $E_3 = 50.0$ and $E_4 = 200.0$; interaction between the two spins is not so strong to cause reversal of the energy levels. Due to the low temperature condition, the thermal equilibrium state is almost concentrated to the ground state $|1\rangle$.

Time evolution of expectation values $\langle S_1^z \rangle$ and $\langle S_2^z \rangle$ are out of phase, due to the energy exchange between the two spins. Time evolution of the expectation values of transverse components of spins is expressed in terms of superposition of time evolution of several components with different frequency. It is a characteristic feature that the relaxation time of longitudinal components and the transverse components are the same order. This is unusual for the *single* spin systems. But as will be seen later, the energy relaxation process of the *coupled* spin system does not coincide with the energy relaxation process of *each* spin.

We show the three dimensional plot of trajectories of $\langle \mathbf{S}_\alpha \rangle = (\langle S_\alpha^x \rangle, \langle S_\alpha^y \rangle, \langle S_\alpha^z \rangle)$ for spin $\alpha = 1, 2$ for time domain $0 \leq gt \leq 500$ in Fig.4.2. For comparison's sake, we show

the corresponding trajectories for the dissipation-less case ($\kappa_1, \kappa_2 = 0$) with the same parameters as in Fig.4.3. Under the resonant condition of the two spins $\omega_1 = \omega_2$, the trajectories of dissipation-less coupled spin system are periodic as in Fig.4.3. We see that the periodic coherent motion is destroyed by the dissipation effect which causes the relaxation to the thermal equilibrium value for the longigudinal components and the decay for the transverse components of spins as in Fig.4.2.

Time evolution of the expectation values for the strong coupling case is shown in Fig.4.4. Parameters are given by $\kappa_1/g = \kappa_2/g = 0.01$, $g_z/g = 1$, $\omega_1/g = \omega_2/g = 0.2$ and $T/g = 0.01$. In this condition, the energy eigenvalues are $E_1 = 5$, $E_2 = -75$, $E_3 = 25$ and $E_4 = 45$, and thus reversal of the energy levels occurs. The ground state is $|2\rangle$. The expectation values of longitudinal spin components relax to the the correct equilibrium even in this strong coupling limit: that is beyond the usual treatment. As is seen from Fig.4.4, when the coupling strength becomes strong, the transverse components of spins behave entirely different form the ordinary situation. Trajectories of the expectation values are shown in Fig.4.5 and the corresponding trajectories for the dissipation-less model are shown in Fig.4.6.

In Fig.4.7, we show results of calculations for the non-resonant condition of two spins. Parameters are given by $\kappa_1/g = \kappa_2/g = 0.01$, $g_z/g = 1$, $\omega_1/g = 0.1$ and $\omega_2/g = 0.2$, for which reversal of energy levels occurs. Temperature is given as $T/g = 0.2$. Damping constants are the same as in Fig.4.4. Trajectories of the expectation values of spins are shown in Fig.4.8. Corresponding trajectories with the dissipation-less model are shown in Fig.4.9. It is interesting to note that even the trajectories for the dissipation-less model are not periodic in this non-resonant condition as we see in Fig.4.9.

To show the advantage of our model, we compare time evolution of the expectation values calculated within the usual relaxation model for the coupled two spin $\frac{1}{2}$ particles. In the usual treatment, time evolution of operators in the damping terms is not determined by the total Hamiltonian of the system but by the Hamiltonian of each subsystems as $S_\alpha^\pm(t) = e^{iH_\alpha t/\hbar} S_\alpha^\pm e^{-iH_\alpha t/\hbar}$ where $H_\alpha = \hbar\omega_\alpha S_\alpha^z$ for spin $\alpha = 1, 2$. The equation of motion derived from the usual damping terms coincides with our equation

of motion only at zero temperature condition and the case without reversal of energy levels. In Fig.4.10, we show the result for the usual relaxation model. The parameters are the same as in Fig.4.7. The apparent difference seen from the figures is that the expectation values do not relax to the correct thermal equilibrium values. The relaxation time of the expectation values are observed to be shorter than that of our model.

Phase relaxation and energy relaxation

Next, we study the phase relaxation process and the energy relaxation process of the coupled system. For this purpose, we define new quantities which characterize relaxation processes of the coupled system with use of $\mathrm{Tr}\rho^2$. We call the quantity $\mathrm{Tr}\rho^2$ as "purity" in this thesis. The purity is often used as a tool to know whether the system is in a pure state or in a mixed state [4]; $\mathrm{Tr}\rho^2 = 1$ for a pure state, and $\mathrm{Tr}\rho^2 \neq 1$ for a mixed state.

The purity in the eigenstate bases is written in the form

$$\mathrm{Tr}\left\{\rho(t)\right\}^2 = \sum_{n,m=1}^{4} \rho_{nm}(t)\rho^*_{nm}(t). \tag{4.4.8}$$

We divide purity into two parts. We define $p_d(t)$ as the partial purity coming from the diagonal elements and $p_o(t)$ as the partial purity coming from the off-diagonal elements, that is,

$$p_d(t) = \sum_n \rho_{nn}(t)\rho^*_{nn}(t), \tag{4.4.9}$$

$$p_o(t) = 2\sum_{n>m} \rho_{nm}(t)\rho^*_{nm}(t). \tag{4.4.10}$$

All elements of the reduced density matrix of group the B (B') and C (C') contribute to p_o. But the elements of the group A contridute both to $p_o(t)$ and $p_o(t)$.

Decay of $p_o(t)$ describes the phase relaxation of the coupled system. In contrast, the meaning of $p_d(t)$ is not trivial. As for the thermal equilibrium, $p_d(t = \infty)$ is a monotonously decreasing function of temperature T as

$$p_d(t=\infty) = \frac{\sum_n e^{-2E_n/k_BT}}{\left(\sum_n e^{-E_n/k_BT}\right)^2}, \tag{4.4.11}$$

where $p_d(t=\infty)=1$ for $T=0$, $p_d(t=\infty)=\frac{1}{4}$ for $T=\infty$, and $p_d(\infty)=\mathrm{Tr}\rho^2(\infty)$. Thus time evolution of $p_d(t)$ is regarded as an index of the coupled system how to reach the thermal equilibrium state, that is, the energy relaxation.

In Fig.4.11 and Fig.4.12, we show time evolution of the quantities $p_d(t)$, $p_o(t)$ at various temperatures. The system parameters of Fig.4.10 and Fig.4.11 are the same as the ones for Fig.4.1 and Fig.4.7, respectively. Qualitatively speaking, time evolution of the purity and the partial purity are not different between Fig.4.10 and Fig.4.11. For the low temperature condition ($T/g=0.01$ and $T/g=0.2$), we see that the purity decreases once and then increases toward the equilibrium value, because $p_o(t)$ decays in time but $p_d(t)$ increases. At higher temperatures $T/g=2.0$, both $p_d(t)$ and $p_o(t)$ decay in the short time region leading to the monotonous decay of the purity. The relaxation time of $p_d(t)$ (energy relaxation) is longer than that of $p_o(t)$ (phase relaxation) at any temperatures.

In Fig.4.13, we show calculated results in the usual treatment for the same parameters as in Fig.4.12. For the usual treatment, both the phase relaxation time and the energy relaxation time are shorter than the ones of our relaxation theory.

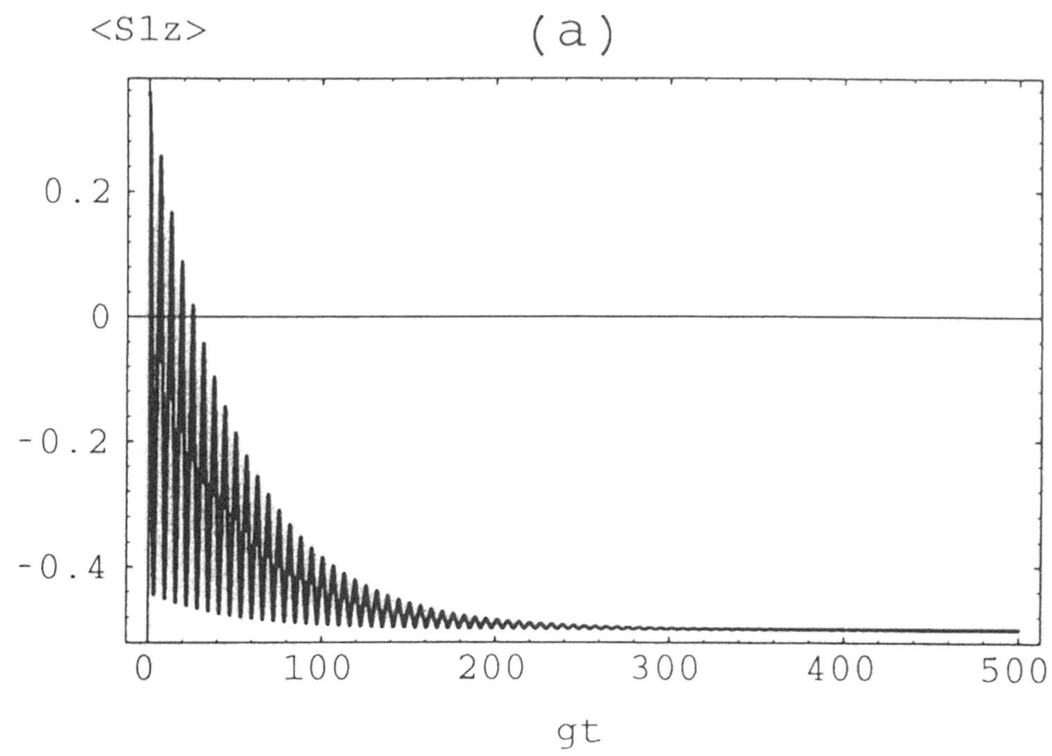

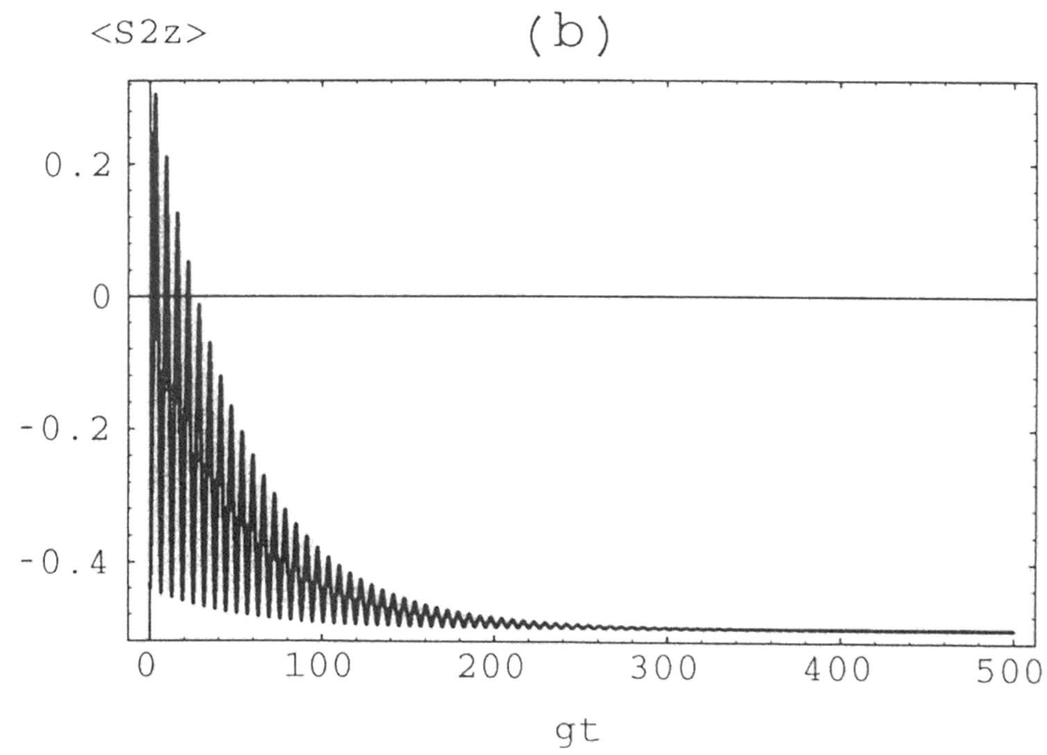

Figure 4.1: Time evolution of expectation values (a) $\langle S_1^z \rangle$ (b) $\langle S_2^z \rangle$ (c) $\langle S_1^x \rangle$ (d) $\langle S_2^x \rangle$ for the case without reversal of the energy levels in scaled time gt from initial condition $\theta_1 = \pi/4$, $\varphi_1 = \pi/2$, $\theta_2 = 5\pi/6$, $\varphi_1 = 5\pi/6$. Parameters are $\kappa_1/g = \kappa_2/g = 0.01$, $g_z/g = 0$, $\omega_1/g = \omega_2/g = 2$ and $T/g = 0.01$.

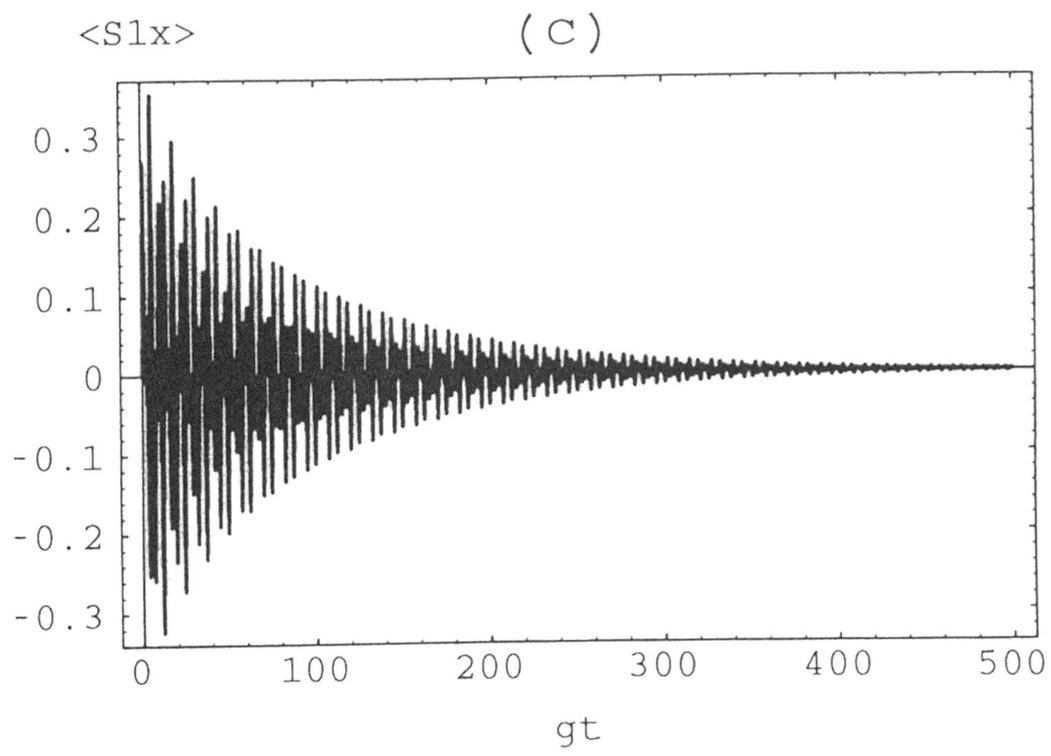

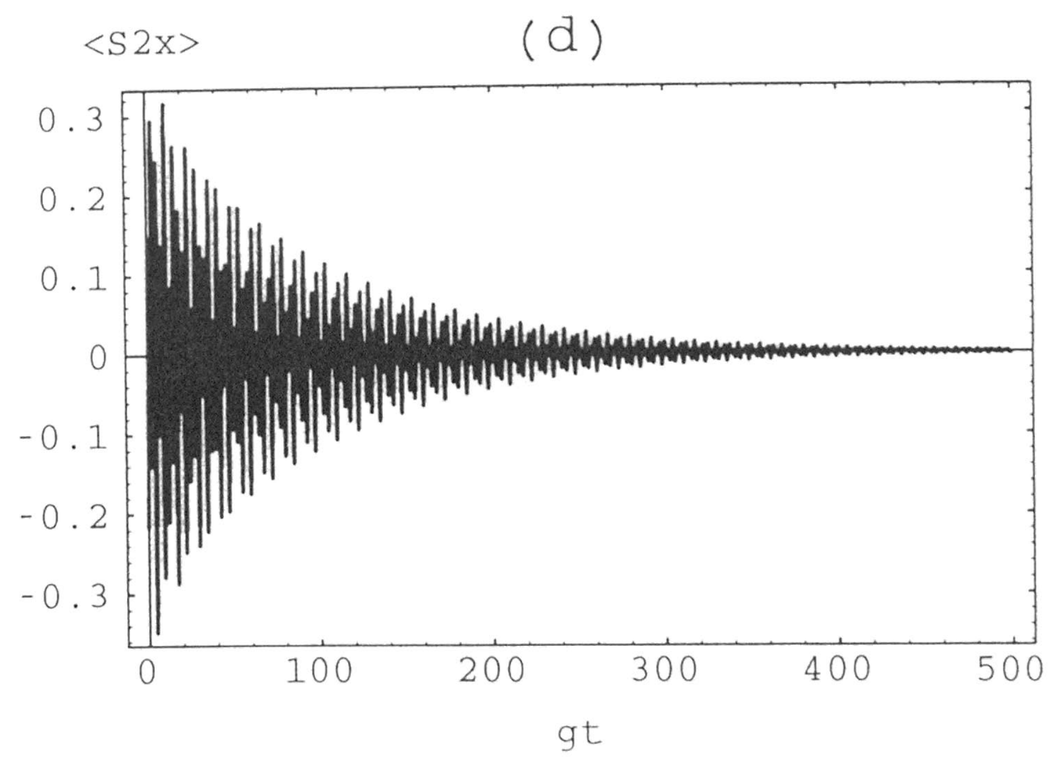

Figure 4.1: – continued.

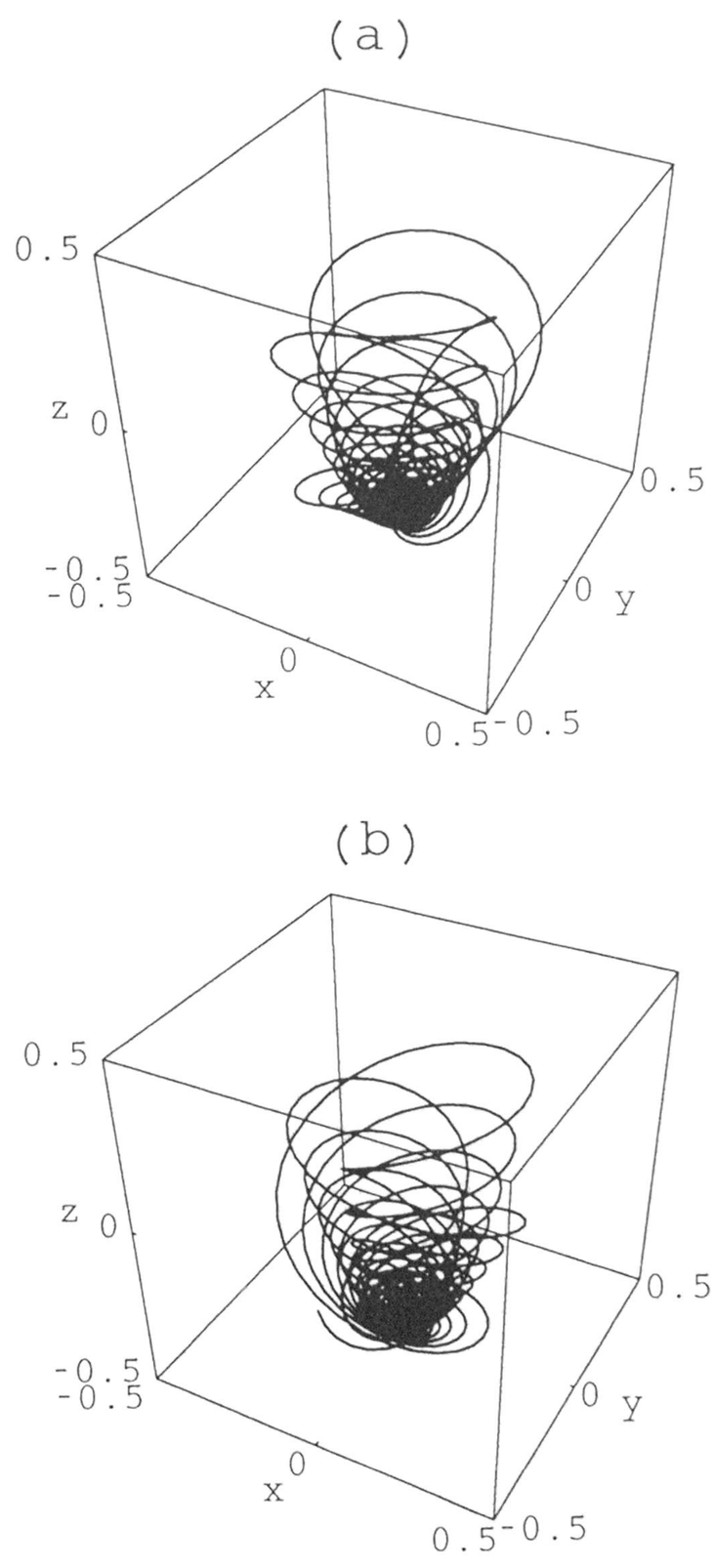

Figure 4.2: Three dimensional plot of trajectories of (a)$\langle \mathbf{S}_1 \rangle$ (b)$\langle \mathbf{S}_2 \rangle$ in time domain $0 \leq gt \leq 500$. Parameters are the same as in Fig.4.1.

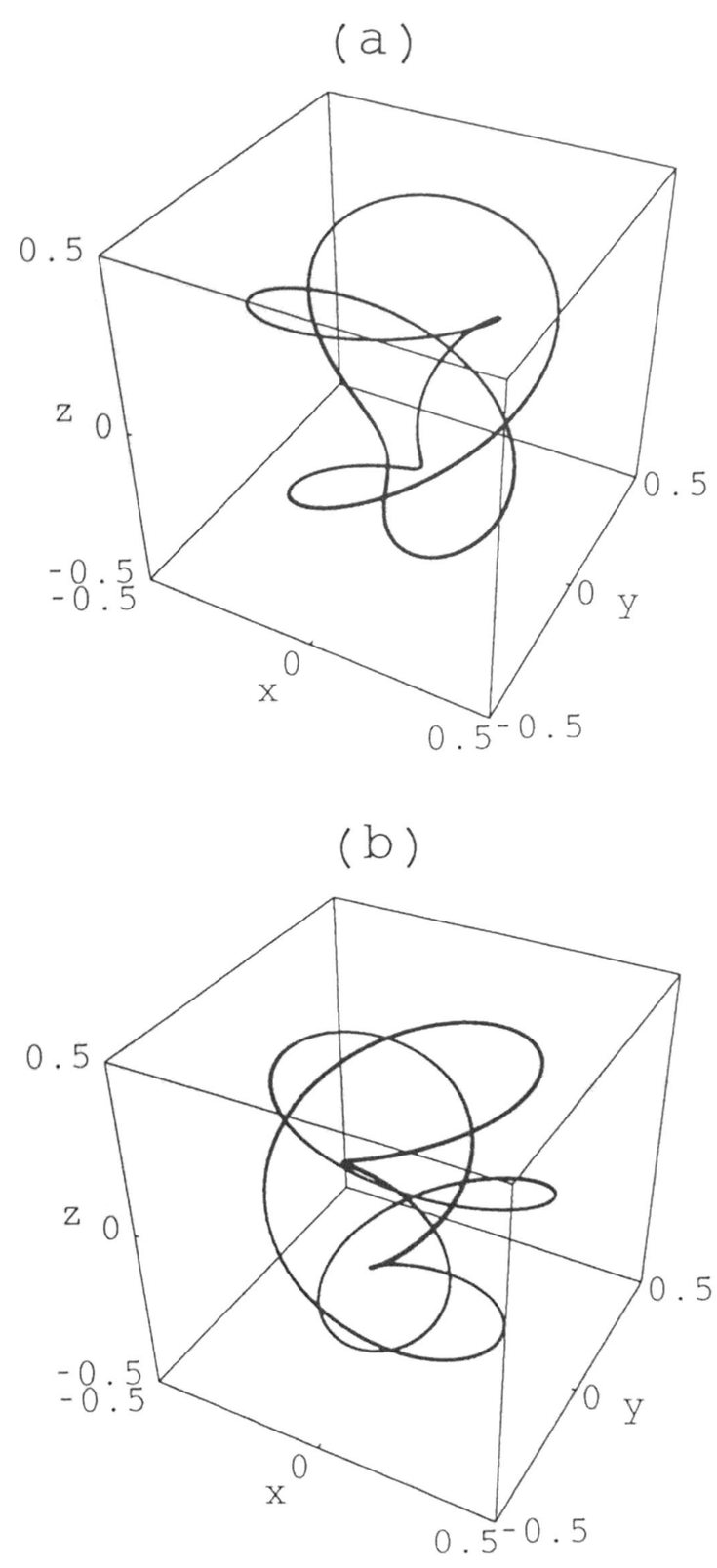

Figure 4.3: Three dimensional plot of trajectories of (a)$\langle \mathbf{S}_1 \rangle$ (b)$\langle \mathbf{S}_2 \rangle$ for the dissipationless case ($\kappa_1, \kappa_2 = 0$) in time domain $0 \leq gt \leq 500$. Parameters of the system variables are the same as in Fig.4.2.

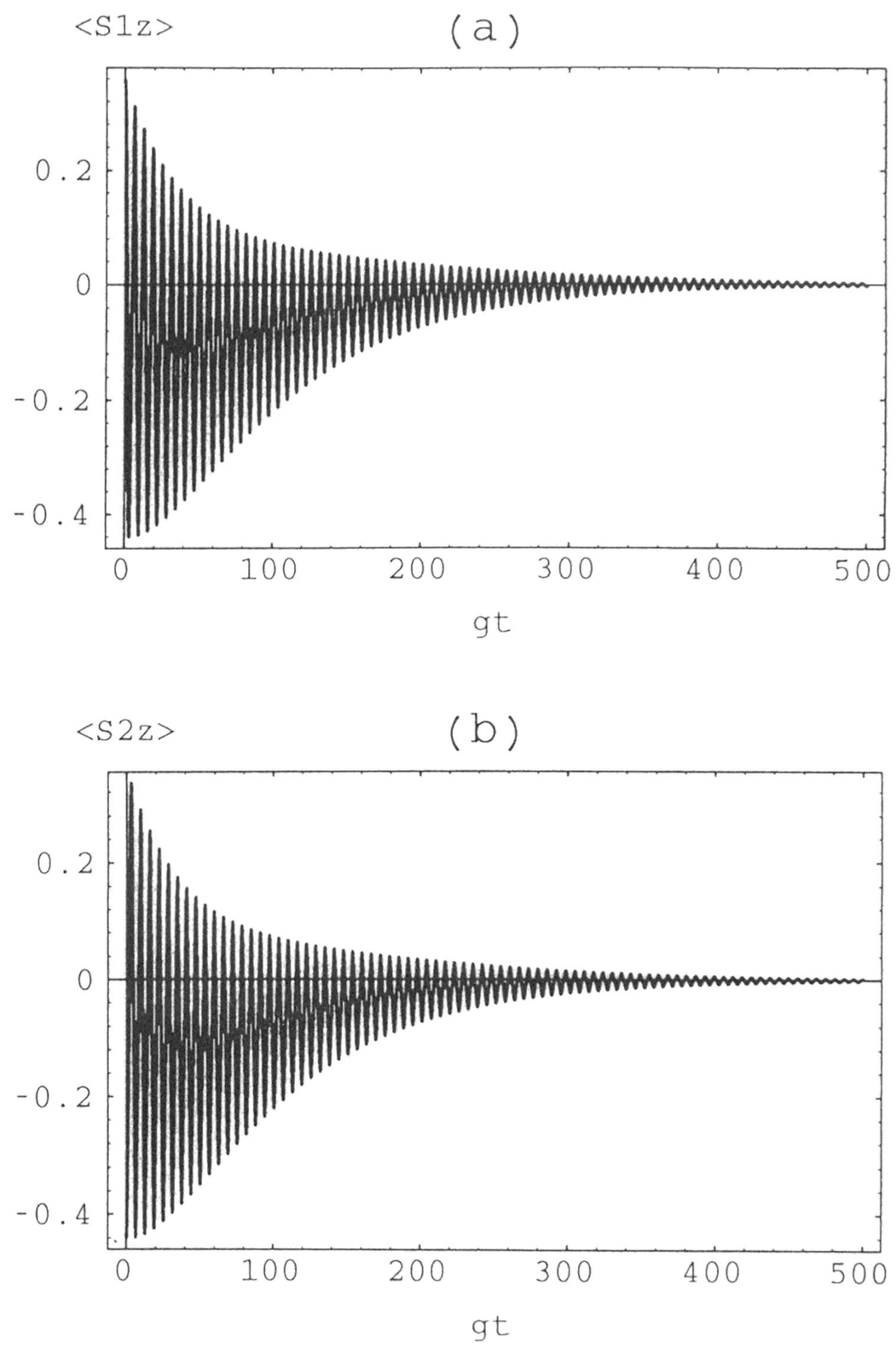

Figure 4.4: Time evolution of expectation values (a) $\langle S_1^z \rangle$ (b) $\langle S_2^z \rangle$ (c) $\langle S_1^x \rangle$ (d) $\langle S_2^x \rangle$ for strong coupling in scaled time gt from initial condition $\theta_1 = \pi/4$, $\varphi_1 = \pi/2$, $\theta_2 = 5\pi/6$, $\varphi_1 = 5\pi/6$. Parameters are $\kappa_1/g = \kappa_2/g = 0.01$, $g_z/g = 1$, $\omega_1/g = \omega_2/g = 0.2$ and $T/g = 0.01$.

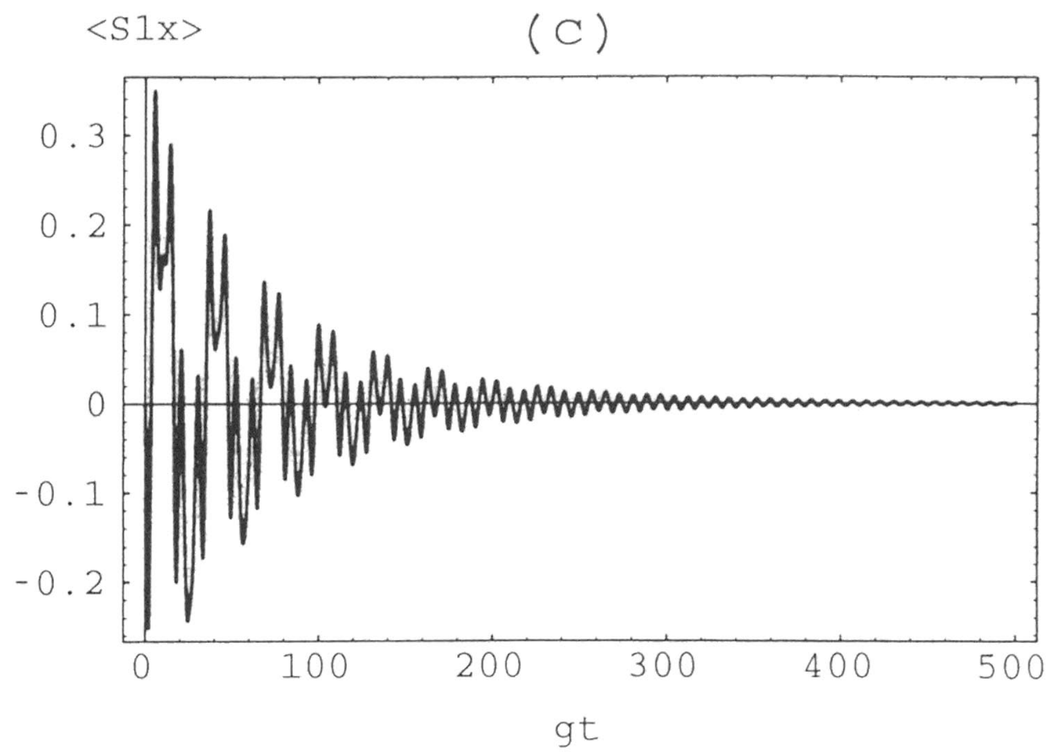

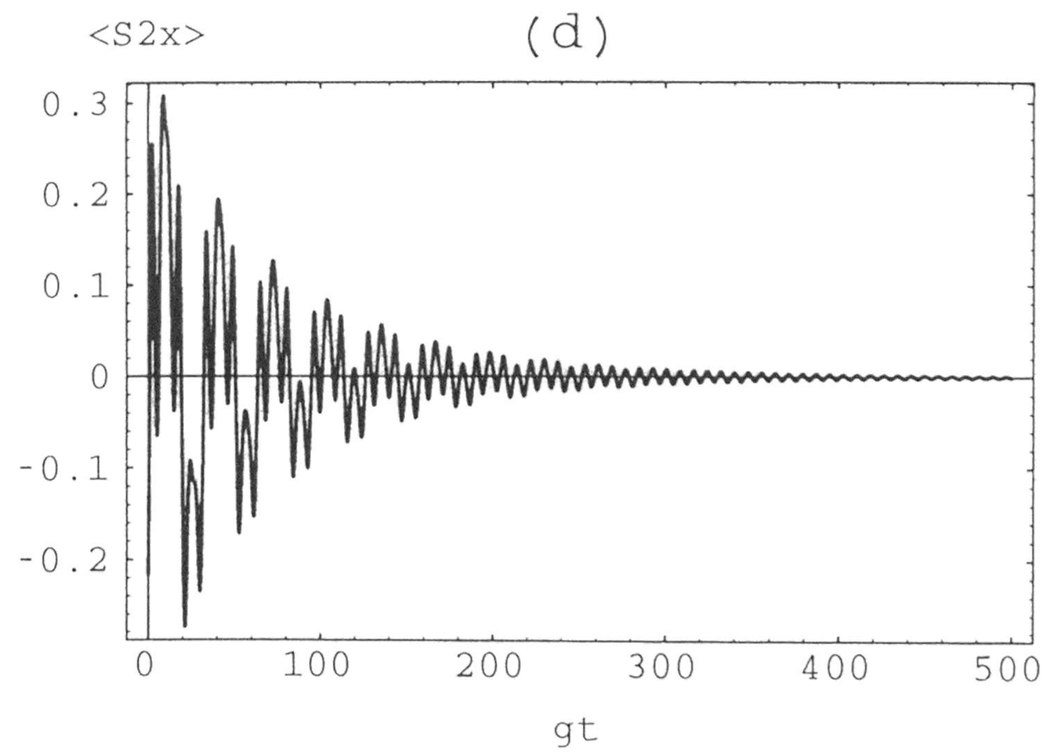

Figure 4.4: – continued.

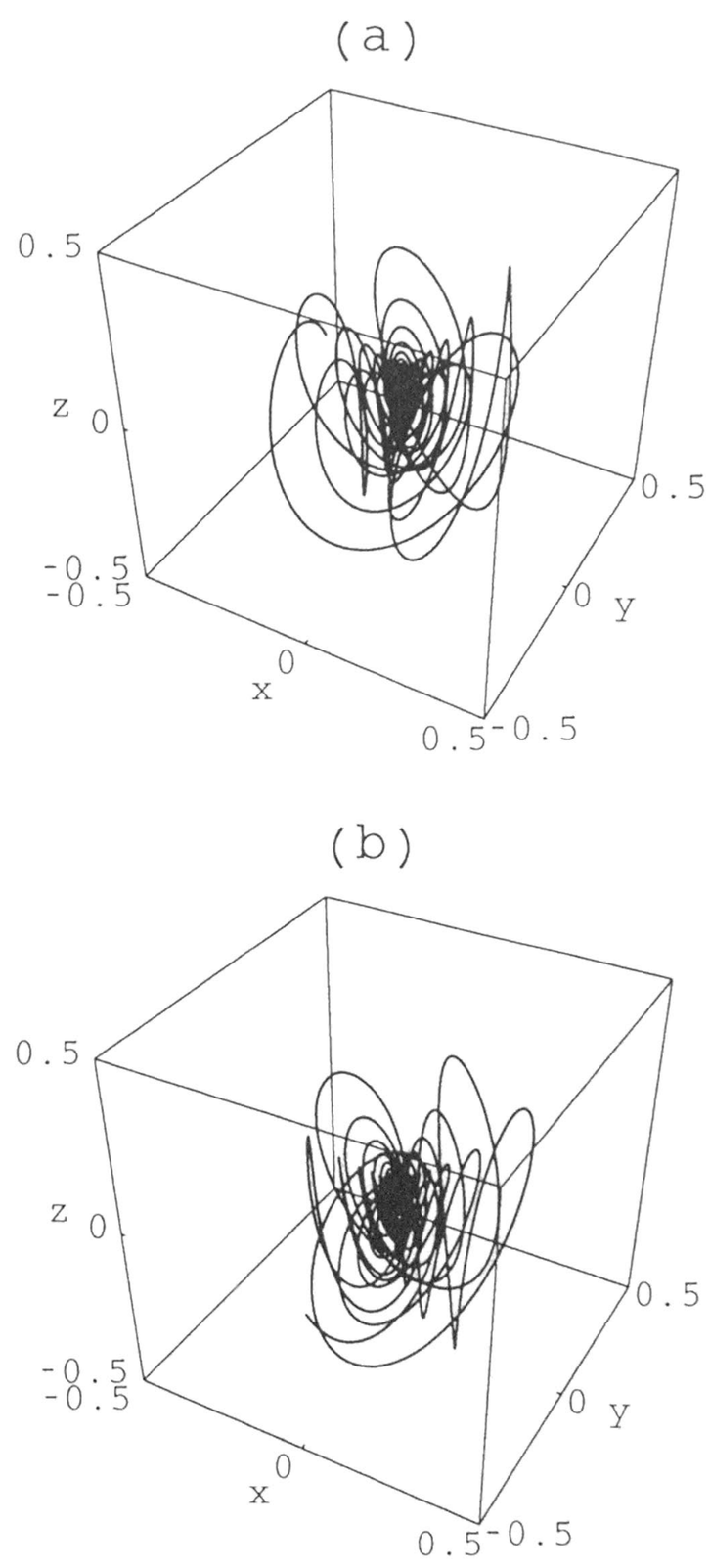

Figure 4.5: Three dimensional plot of trajectories of (a)$\langle \mathbf{S}_1 \rangle$ (b)$\langle \mathbf{S}_2 \rangle$ in time domain $0 \leq gt \leq 500$. Parameters are the same as in Fig.4.4.

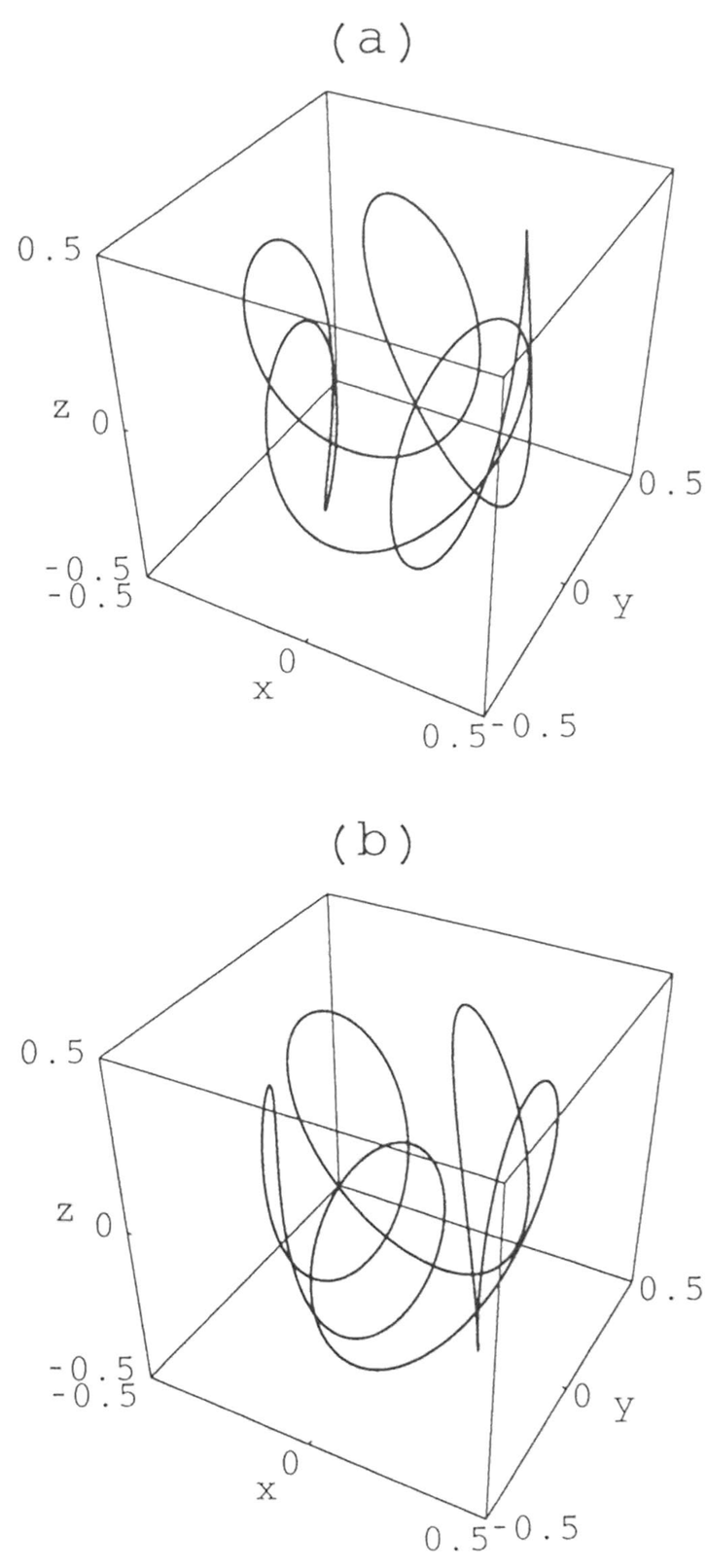

Figure 4.6: Three dimensional plot of trajectories of (a)$\langle \mathbf{S}_1 \rangle$ (b)$\langle \mathbf{S}_2 \rangle$ for the dissipationless case ($\kappa_1, \kappa_2 = 0$) in time domain $0 \leq gt \leq 500$. Parameters of the system variables are the same as in Fig.4.5.

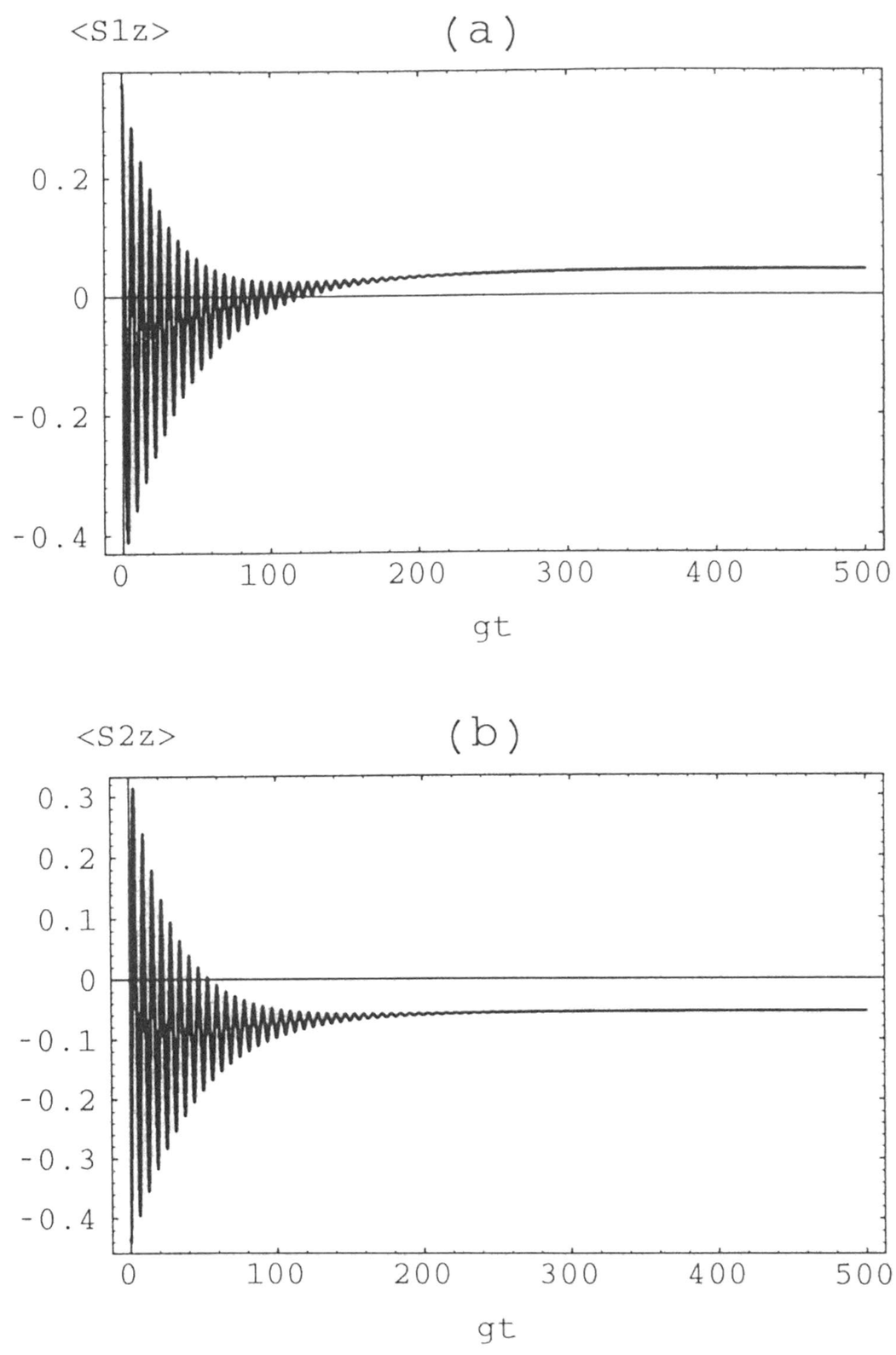

Figure 4.7: Time evolution of expectation values (a) $\langle S_1^z \rangle$ (b) $\langle S_2^z \rangle$ (c) $\langle S_1^x \rangle$ (d) $\langle S_2^x \rangle$ for non-resonant spins from initial condition $\theta_1 = \pi/4$, $\varphi_1 = \pi/2$, $\theta_2 = 5\pi/6$, $\varphi_1 = 5\pi/6$. Parameters are $\kappa_1/g = \kappa_2/g = 0.01$, $g_z/g = 1$, $\omega_1/g = 0.1$, $\omega_2/g = 0.2$ and $T/g = 0.2$.

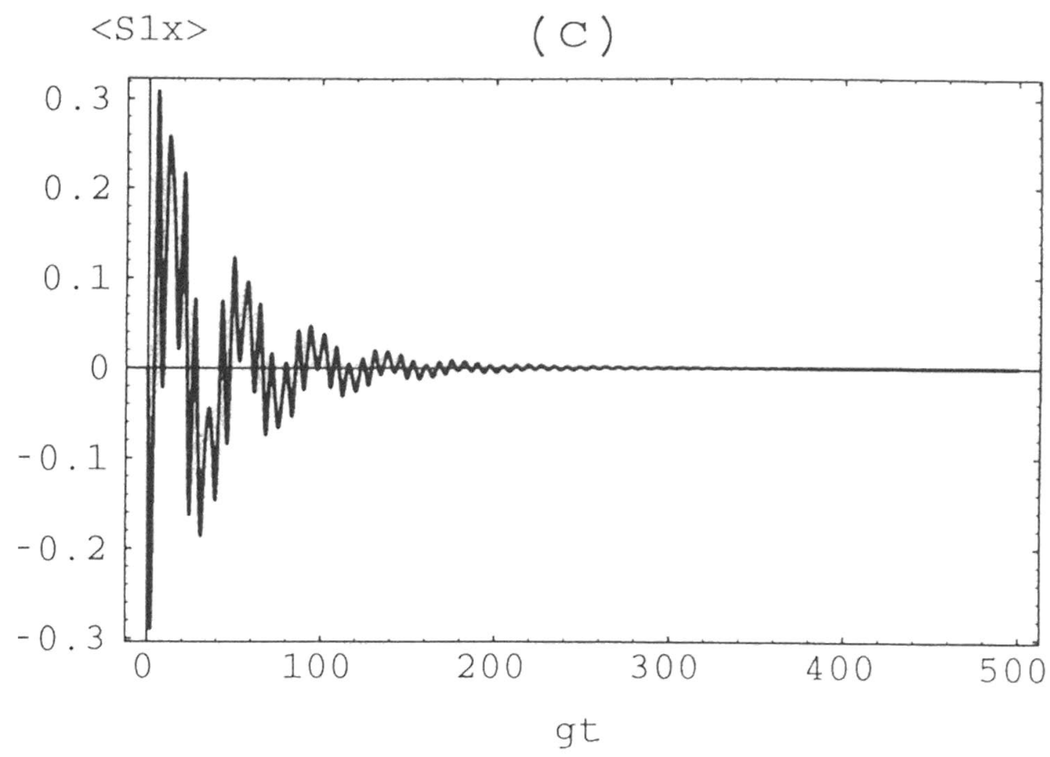

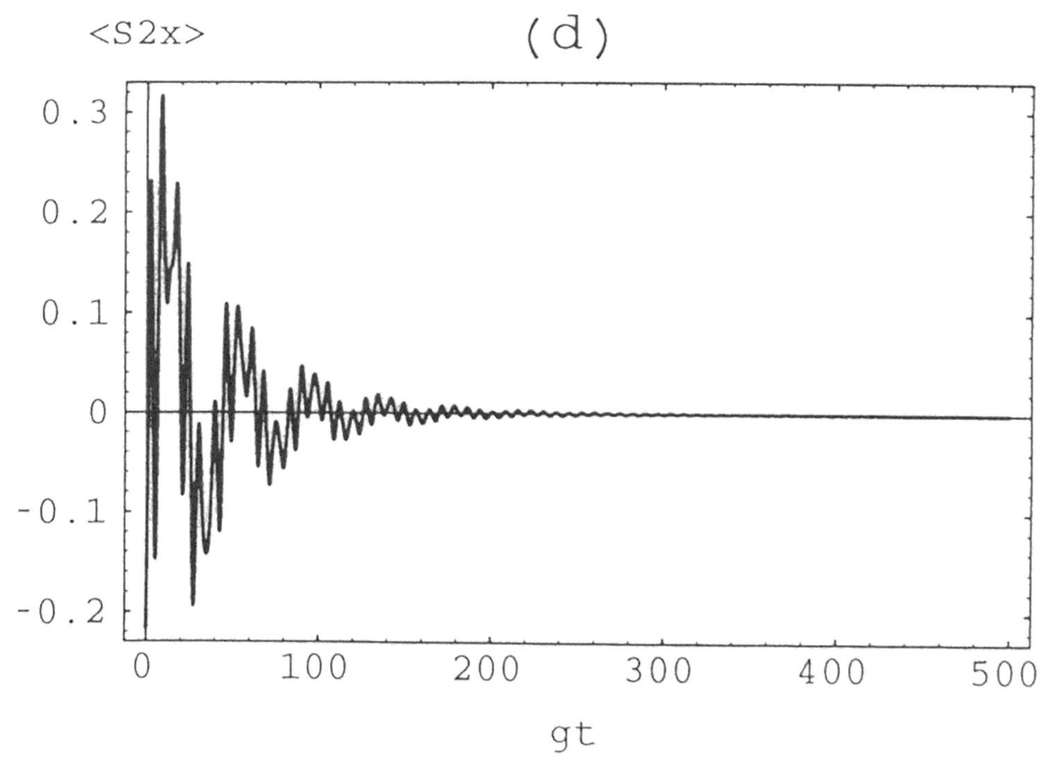

Figure 4.7: – continued.

(a)

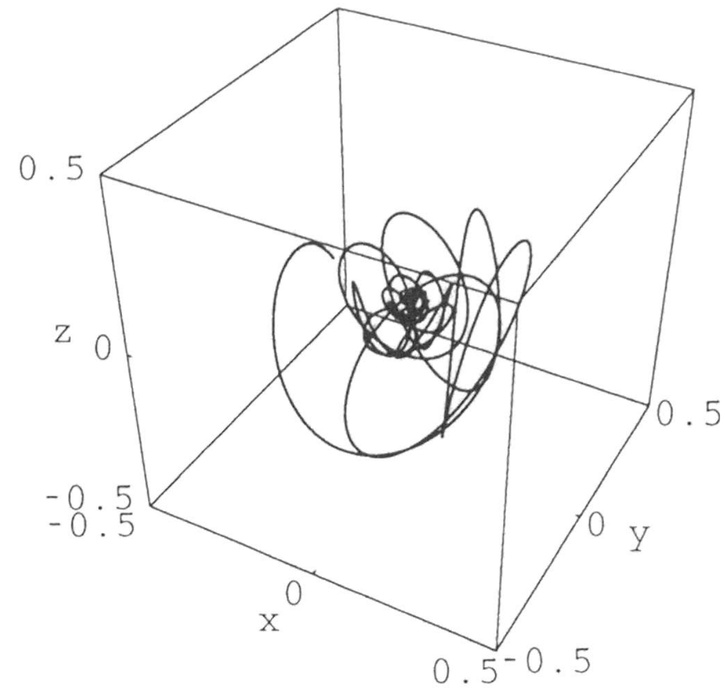

(b)

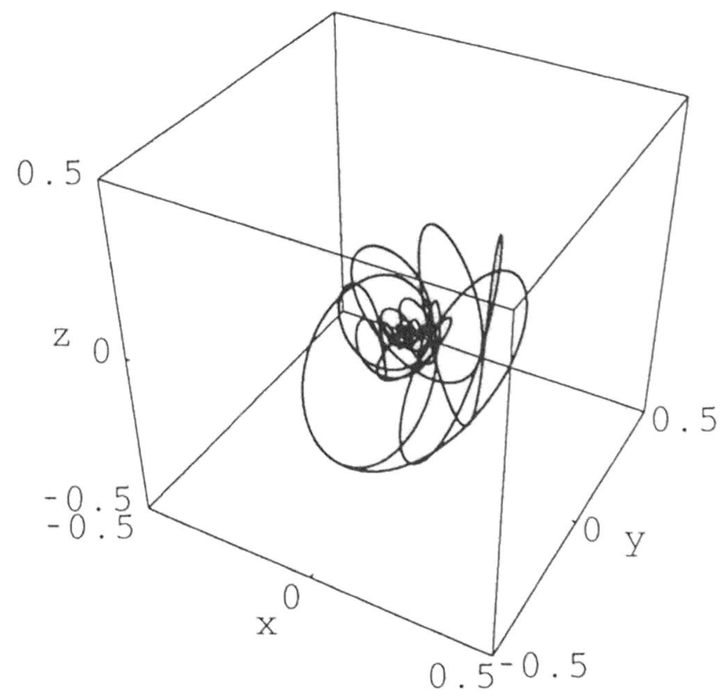

Figure 4.8: Three dimensional plot of trajectories of (a)$\langle \mathbf{S}_1 \rangle$ (b)$\langle \mathbf{S}_2 \rangle$ in time domain $0 \leq gt \leq 500$. Parameters are the same as in Fig.4.7.

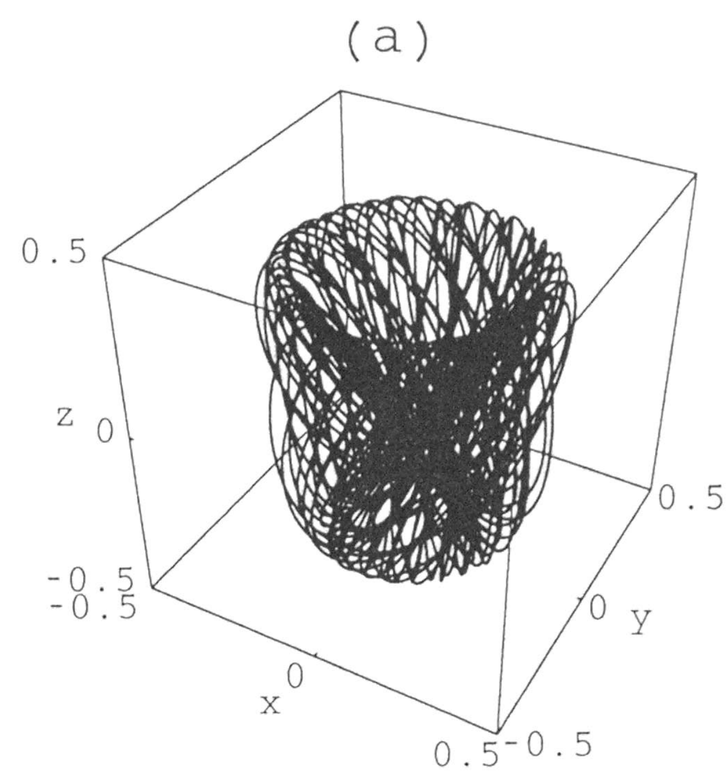

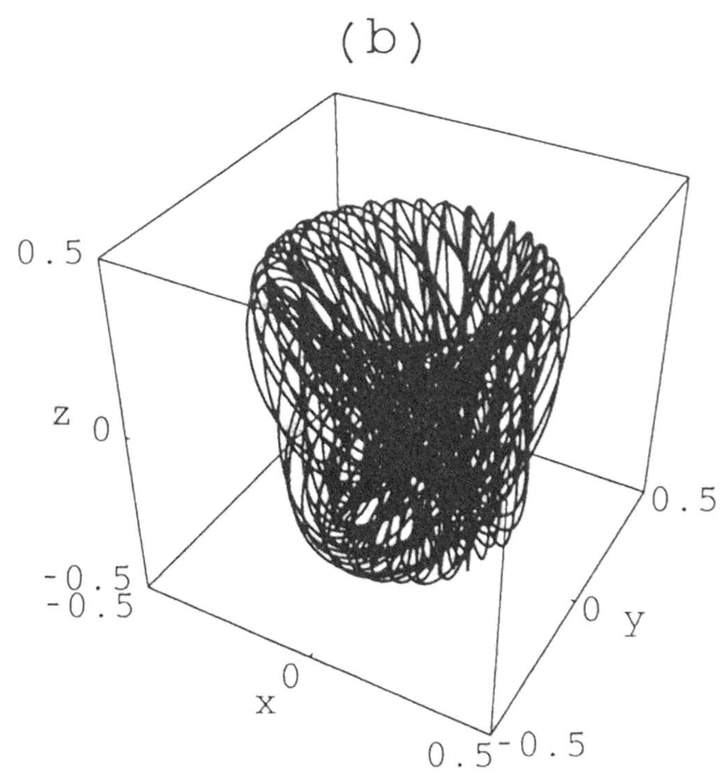

Figure 4.9: Three dimensional plot of trajectories of (a)$\langle \mathbf{S}_1 \rangle$ (b)$\langle \mathbf{S}_2 \rangle$ for the dissipationless case ($\kappa_1, \kappa_2 = 0$) in time domain $0 \leq gt \leq 500$. Parameters of the system variables are the same as in Fig.4.8.

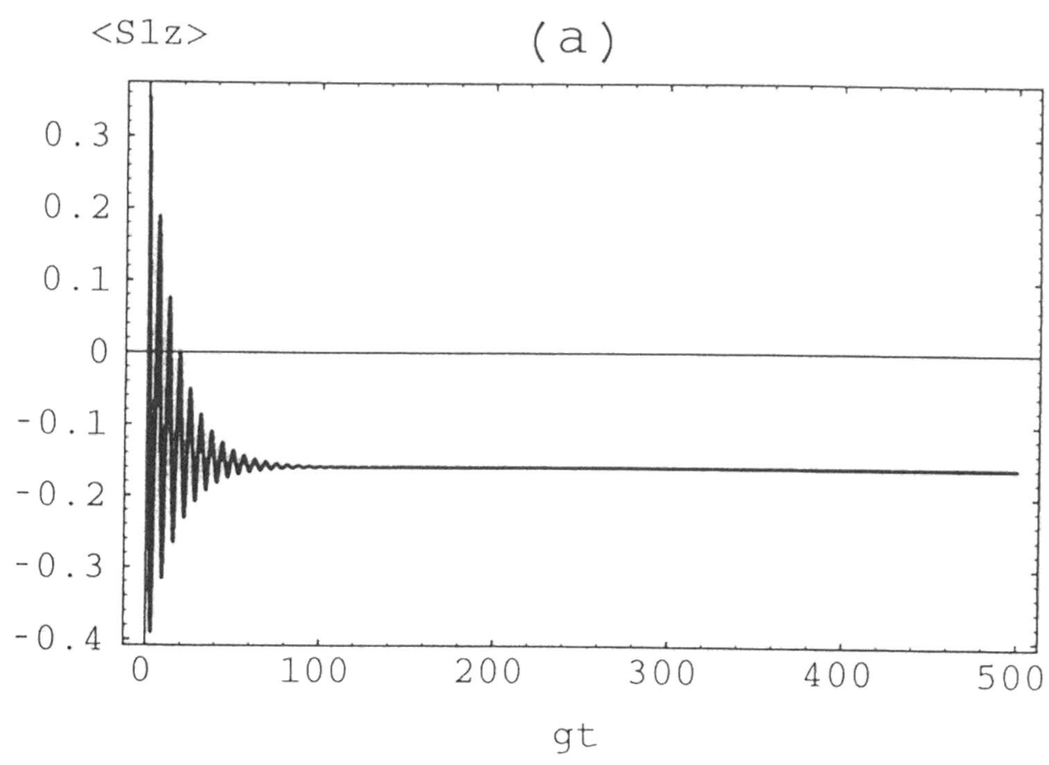

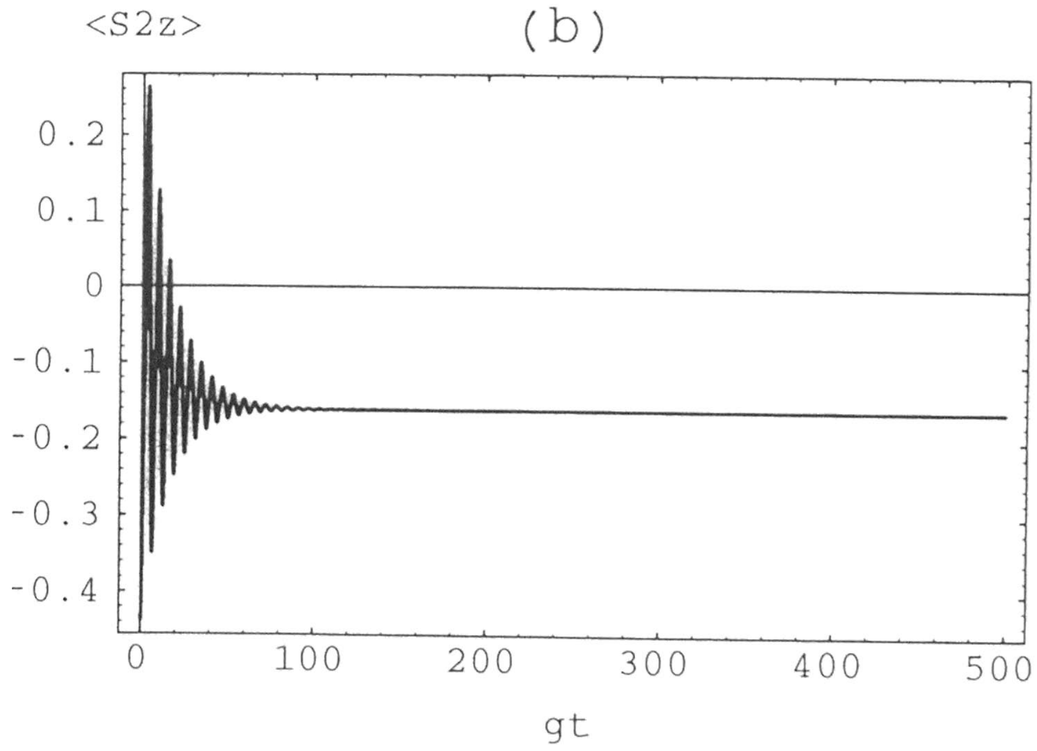

Figure 4.10: Time evolution of expectation values (a) $\langle S_1^z \rangle$ (b) $\langle S_2^z \rangle$ (c) $\langle S_1^x \rangle$ (d) $\langle S_2^x \rangle$ calculated within the usual relaxation model. The initial condition and the parameters are the same as in Fig.4.7.

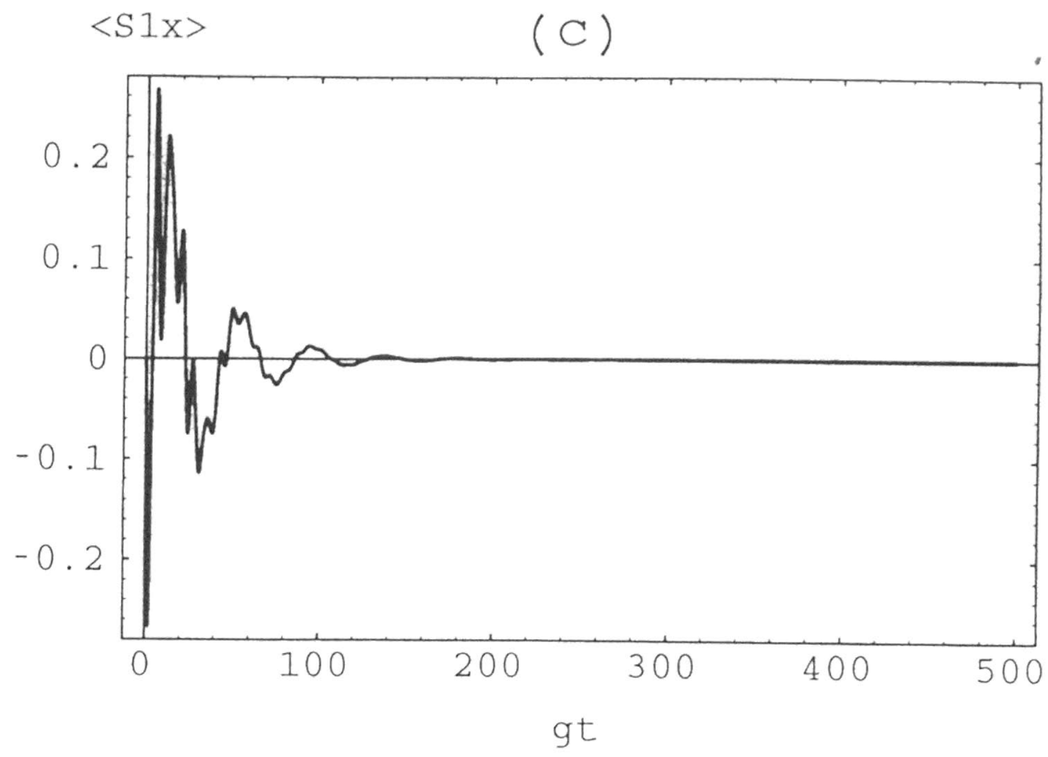

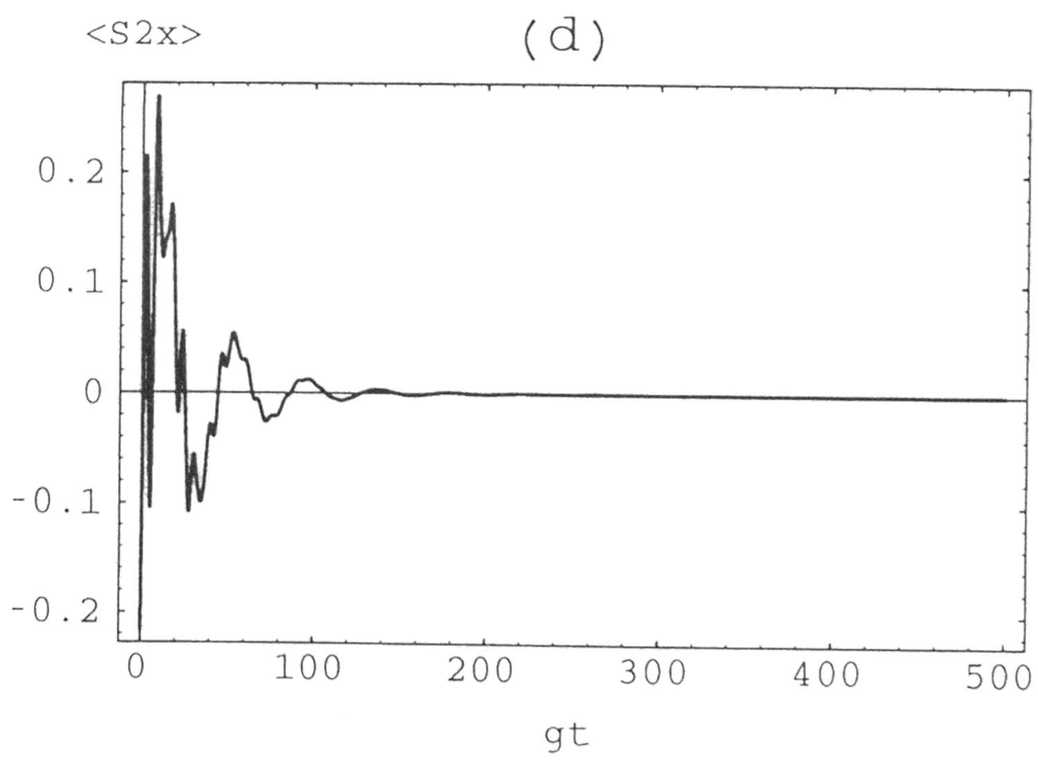

Figure 4.10: – continued.

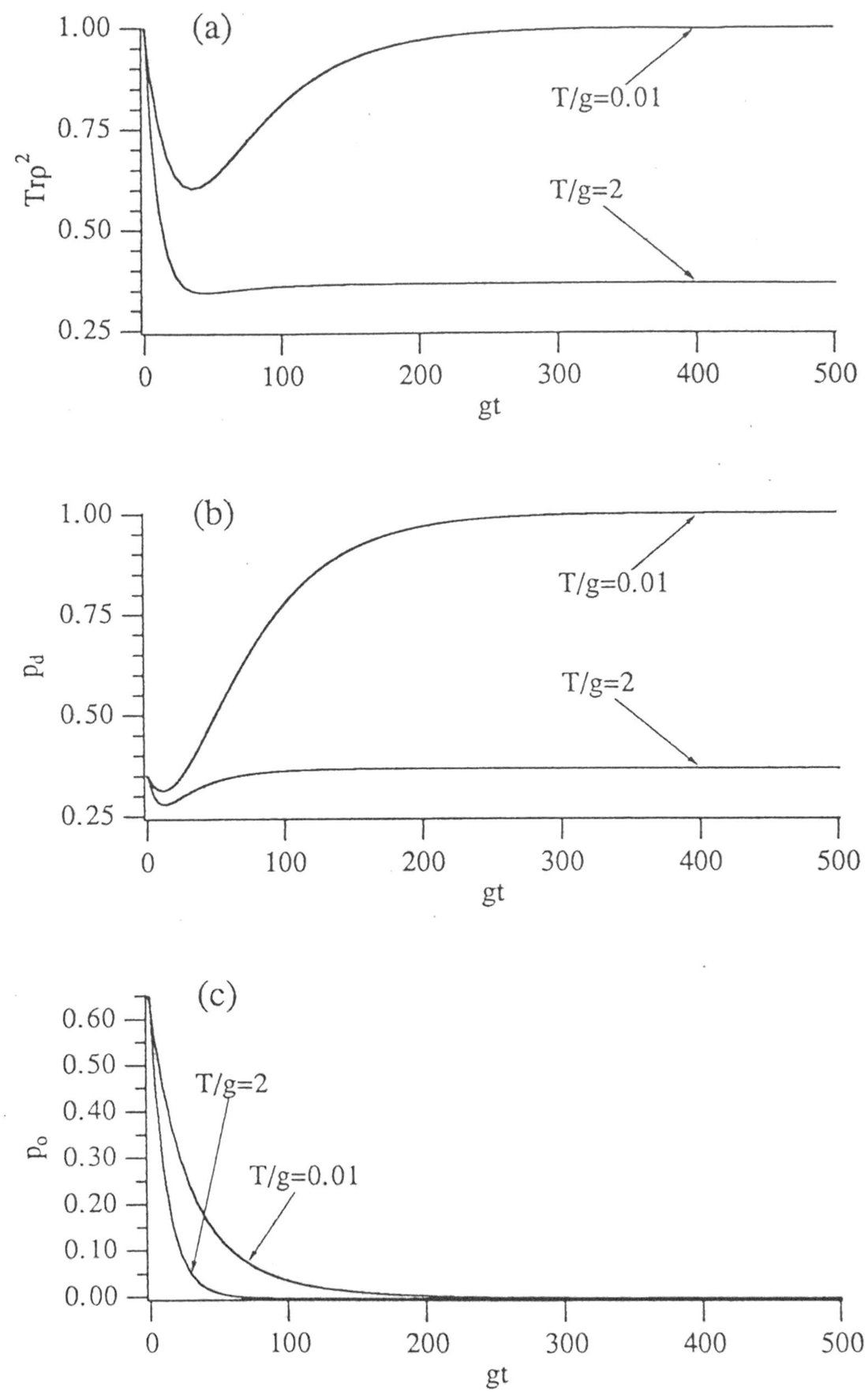

Figure 4.11: Time evolution of (a) the purity $\mathrm{Tr}\rho^2$, (b) the partial purity coming from the diagonal elements p_d and (c) the partial purity coming from the off-diagonal elements p_o at several temperatures $T/g = 0.01, 2$. Parameters are the same as in Fig.4.1.

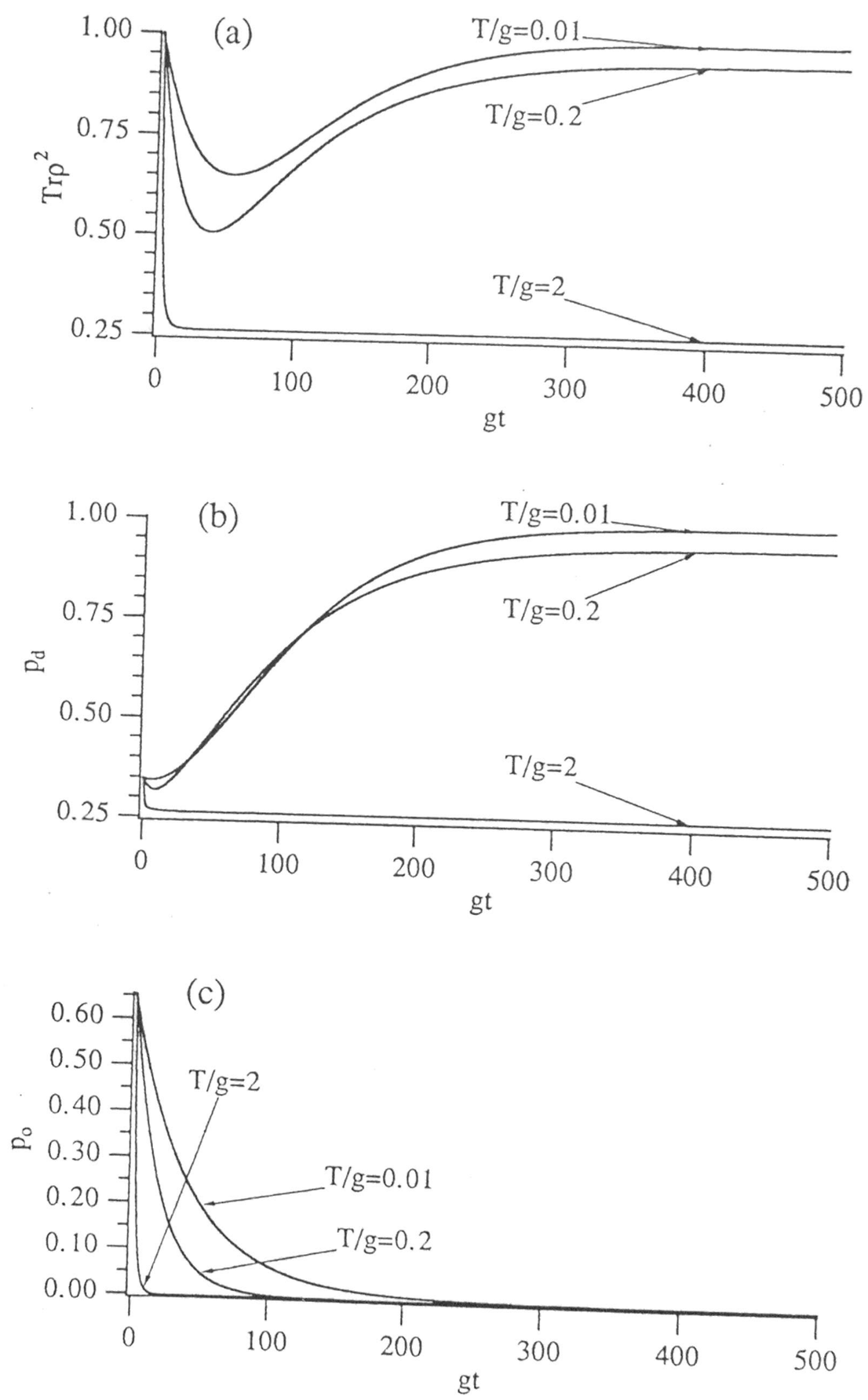

Figure 4.12: Time evolution of (a) the purity $\mathrm{Tr}\rho^2$, (b) the partial purity coming from the diagonal elements p_d and (c) the partial purity coming from the off-diagonal elements p_o at several temperatures $T/g = 0.01, 0.2, 2$. Parameters are the same as in Fig.4.7.

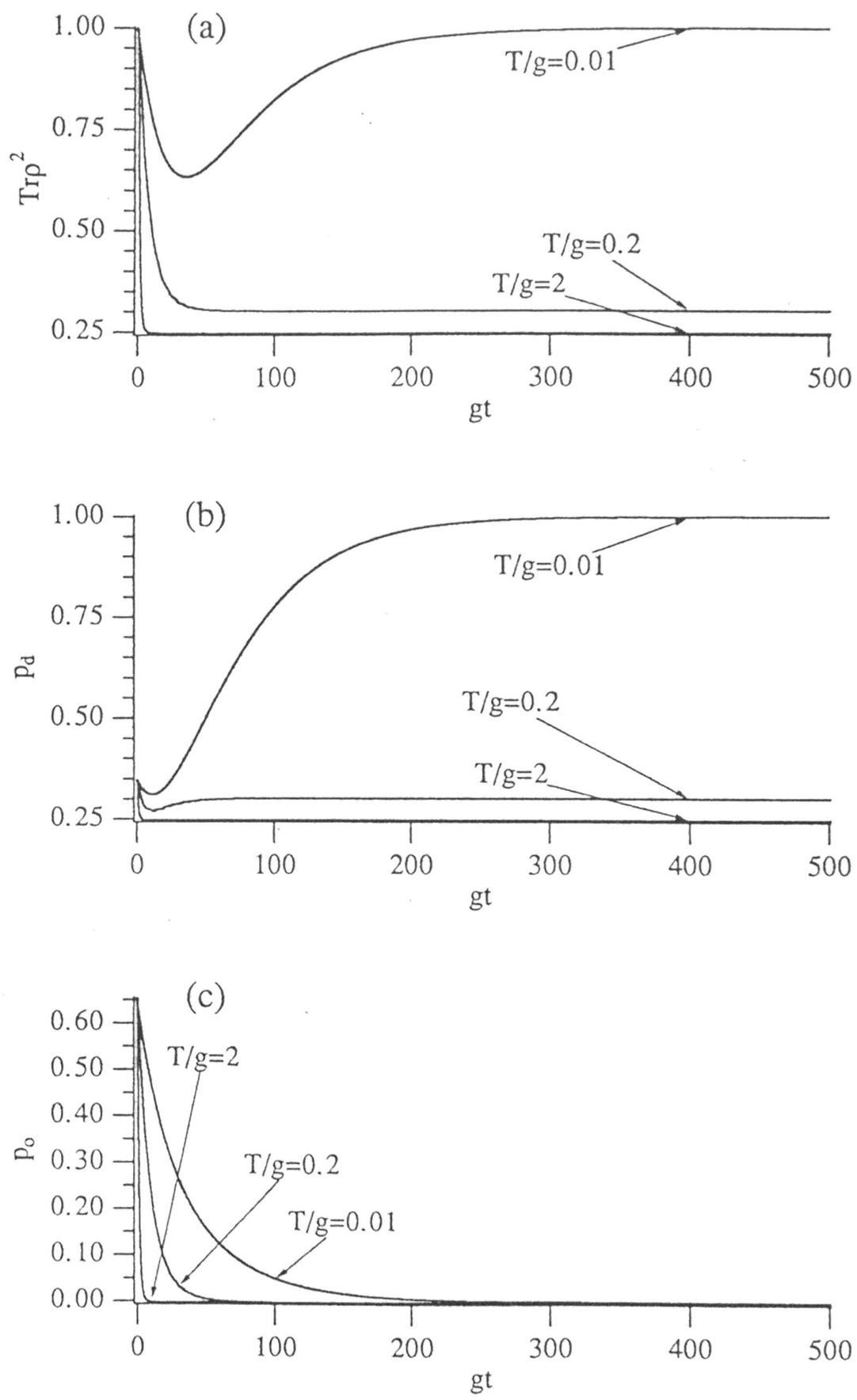

Figure 4.13: Time evolution of (a) the purity $\mathrm{Tr}\rho^2$, (b) the partial purity coming from the diagonal elements p_d and (c) the partial purity coming from the off-diagonal elements p_o in the usual treatment at several temperatures $T/g = 0.01, 0.2, 2$. Parameters are the same as in Fig.4.12.

4.5 Short Summary

We have obtained the master equation which describes the quantum dynamics of the strongly coupled two spin $\frac{1}{2}$ particles system toward the thermal equilibrium by TCL formalism. For this model, we can introduce the Raman-like dissipation mechanisms in addition to the normal first order dissipation mechanisms. We have derived the solvable equations for the elements of the reduced density matrix by expanding the master equation in terms of the eigenstates of the coupled system. These are three independent vector equations: It was found that the effects of the dissipation mechanisms introduced in this paper do not cause any mixing of the expansion coefficients among other groups. The phase relaxation process and the energy relaxation process of the strongly coupled system were also fully investigated.

This model describes the phase relaxation and the energy relaxation of the strongly coupled system. Application of our theory to actual physical problems may afford certain insight into the relaxation processes of strongly coupled systems.

Appendix

4.A Matrix elements

The explicit representations of the coefficient matrices for coherent motion in (4.3.24) are given as

$$\boldsymbol{L}^A = \begin{pmatrix} 0 & 0 & 0 & 0 & 0 & 0 \\ 0 & 0 & 0 & 0 & 0 & 0 \\ 0 & 0 & -\epsilon^{32} & 0 & 0 & 0 \\ 0 & 0 & 0 & \epsilon^{32} & 0 & 0 \\ 0 & 0 & 0 & 0 & 0 & 0 \\ 0 & 0 & 0 & 0 & 0 & 0 \end{pmatrix}, \tag{4.A.1}$$

$$\boldsymbol{L}^B = \begin{pmatrix} -\epsilon^{21} & 0 & 0 & 0 \\ 0 & -\epsilon^{31} & 0 & 0 \\ 0 & 0 & -\epsilon^{42} & 0 \\ 0 & 0 & 0 & -\epsilon^{43} \end{pmatrix} \tag{4.A.2}$$

and

$$\boldsymbol{L}^C = -\epsilon^{41}. \tag{4.A.3}$$

The matrices of the damping term in (4.3.24) originated from (4.3.2) are of the form

$$\boldsymbol{Q}^A_\alpha = \begin{pmatrix} A^1_\alpha & A^2_\alpha & A^3_\alpha & A^3_\alpha & A^4_\alpha & 0 \\ A^5_\alpha & A^6_\alpha & A^7_\alpha & A^7_\alpha & 0 & A^8_\alpha \\ A^9_\alpha & A^{10}_\alpha & A^{11}_\alpha & 0 & A^7_\alpha & A^{12}_\alpha \\ A^9_\alpha & A^{10}_\alpha & 0 & A^{11}_\alpha & A^7_\alpha & A^{12}_\alpha \\ A^{13}_\alpha & 0 & A^{10}_\alpha & A^{10}_\alpha & A^{14}_\alpha & A^{15}_\alpha \\ 0 & A^{16}_\alpha & A^{17}_\alpha & A^{17}_\alpha & A^{18}_\alpha & A^{19}_\alpha \end{pmatrix}, \tag{4.A.4}$$

$$\boldsymbol{Q}_{\alpha}^{B} = \begin{pmatrix} B_{\alpha}^{1} & B_{\alpha}^{2} & B_{\alpha}^{3} & B_{\alpha}^{4} \\ B_{\alpha}^{5} & B_{\alpha}^{6} & B_{\alpha}^{7} & B_{\alpha}^{8} \\ B_{\alpha}^{9} & B_{\alpha}^{10} & B_{\alpha}^{11} & B_{\alpha}^{2} \\ B_{\alpha}^{12} & B_{\alpha}^{13} & B_{\alpha}^{5} & B_{\alpha}^{14} \end{pmatrix} \tag{4.A.5}$$

and

$$\boldsymbol{Q}_{\alpha}^{C} = C_{\alpha} \tag{4.A.6}$$

where

$$A_{\alpha}^{1} = -2\left\{\left(f_{\alpha}^{1}\right)^{2}\hat{n}_{1}\left(\epsilon_{21}\right) - \left(f_{\alpha}^{2}\right)^{2}\hat{n}_{1}\left(\epsilon_{31}\right)\right\}, \tag{4.A.7}$$

$$A_{\alpha}^{2} = 2\left(f_{\alpha}^{1}\right)^{2}\hat{n}_{2}\left(\epsilon_{21}\right), \tag{4.A.8}$$

$$A_{\alpha}^{3} = f_{\alpha}^{1}f_{\alpha}^{2}\left\{\hat{n}_{2}\left(\epsilon_{21}\right) + \hat{n}_{2}\left(\epsilon_{31}\right)\right\}, \tag{4.A.9}$$

$$A_{\alpha}^{4} = 2\left(f_{\alpha}^{2}\right)^{2}\hat{n}_{2}\left(\epsilon_{31}\right), \tag{4.A.10}$$

$$A_{\alpha}^{5} = 2\left(f_{\alpha}^{1}\right)^{2}\hat{n}_{1}\left(\epsilon_{21}\right), \tag{4.A.11}$$

$$A_{\alpha}^{6} = -2\left\{\left(f_{\alpha}^{1}\right)^{2}\hat{n}_{2}\left(\epsilon_{21}\right) + \left(f_{\alpha}^{3}\right)^{2}\hat{n}_{1}\left(\epsilon_{42}\right)\right\}, \tag{4.A.12}$$

$$A_{\alpha}^{7} = -f_{\alpha}^{1}f_{\alpha}^{2}\hat{n}_{2}\left(\epsilon_{31}\right) - f_{\alpha}^{3}f_{\alpha}^{4}\hat{n}_{1}\left(\epsilon_{43}\right), \tag{4.A.13}$$

$$A_{\alpha}^{8} = 2\left(f_{\alpha}^{3}\right)^{2}\hat{n}_{2}\left(\epsilon_{42}\right), \tag{4.A.14}$$

$$A_{\alpha}^{9} = f_{\alpha}^{1}f_{\alpha}^{2}\left\{\hat{n}_{1}\left(\epsilon_{21}\right) + \hat{n}_{1}\left(\epsilon_{31}\right)\right\}, \tag{4.A.15}$$

$$A_{\alpha}^{10} = -f_{\alpha}^{1}f_{\alpha}^{2}\hat{n}_{2}\left(\epsilon_{21}\right) - f_{\alpha}^{3}f_{\alpha}^{4}\hat{n}_{1}\left(\epsilon_{42}\right), \tag{4.A.16}$$

$$A_{\alpha}^{11} = -\left(f_{\alpha}^{1}\right)^{2}\hat{n}_{2}\left(\epsilon_{21}\right) - \left(f_{\alpha}^{2}\right)^{2}\hat{n}_{2}\left(\epsilon_{31}\right) - \left(f_{\alpha}^{3}\right)^{2}\hat{n}_{1}\left(\epsilon_{42}\right) - \left(f_{\alpha}^{4}\right)^{2}\hat{n}_{1}\left(\epsilon_{43}\right), \tag{4.A.17}$$

$$A_{\alpha}^{12} = f_{\alpha}^{3}f_{\alpha}^{4}\left\{\hat{n}_{2}\left(\epsilon_{42}\right) + \hat{n}_{2}\left(\epsilon_{43}\right)\right\}, \tag{4.A.18}$$

$$A_{\alpha}^{13} = 2\left(f_{\alpha}^{2}\right)^{2}\hat{n}_{1}\left(\epsilon_{31}\right), \tag{4.A.19}$$

$$A_{\alpha}^{14} = -2\left\{\left(f_{\alpha}^{2}\right)^{2}\hat{n}_{2}\left(\epsilon_{31}\right) + \left(f_{\alpha}^{4}\right)^{2}\hat{n}_{1}\left(\epsilon_{43}\right)\right\}, \tag{4.A.20}$$

$$A_{\alpha}^{15} = 2\left(f_{\alpha}^{4}\right)^{2}\hat{n}_{2}\left(\epsilon_{43}\right), \tag{4.A.21}$$

$$A_{\alpha}^{16} = 2\left(f_{\alpha}^{3}\right)^{2}\hat{n}_{1}\left(\epsilon_{42}\right), \tag{4.A.22}$$

$$A_{\alpha}^{17} = f_{\alpha}^{3}f_{\alpha}^{4}\left\{\hat{n}_{1}\left(\epsilon_{42}\right) + \hat{n}_{1}\left(\epsilon_{43}\right)\right\}, \tag{4.A.23}$$

$$A_{\alpha}^{18} = 2\left(f_{\alpha}^{4}\right)^{2}\hat{n}_{1}\left(\epsilon_{43}\right), \tag{4.A.24}$$

$$A_{\alpha}^{19} = -2\left\{\left(f_{\alpha}^{3}\right)^{2}\hat{n}_{2}\left(\epsilon_{42}\right) - \left(f_{\alpha}^{4}\right)^{2}\hat{n}_{2}\left(\epsilon_{43}\right)\right\}, \tag{4.A.25}$$

$$
\begin{aligned}
B_\alpha^1 &= -\left(f_\alpha^1\right)^2\left\{\hat{n}_1\left(\epsilon_{21}\right)+\hat{n}_2\left(\epsilon_{21}\right)\right\}-\left(f_\alpha^2\right)^2\hat{n}_1\left(\epsilon_{31}\right)-\left(f_\alpha^3\right)^2\hat{n}_1\left(\epsilon_{42}\right), && (4.A.26)\\
B_\alpha^2 &= -f_\alpha^1 f_\alpha^2\hat{n}_2\left(\epsilon_{31}\right)-f_\alpha^3 f_\alpha^4\hat{n}_1\left(\epsilon_{43}\right), && (4.A.27)\\
B_\alpha^3 &= f_\alpha^1 f_\alpha^3\left\{\hat{n}_2\left(\epsilon_{21}\right)+\hat{n}_2\left(\epsilon_{42}\right)\right\}, && (4.A.28)\\
B_\alpha^4 &= f_\alpha^2 f_\alpha^3\left\{\hat{n}_2\left(\epsilon_{31}\right)+\hat{n}_2\left(\epsilon_{42}\right)\right\}, && (4.A.29)\\
B_\alpha^5 &= -f_\alpha^1 f_\alpha^2\hat{n}_2\left(\epsilon_{21}\right)-f_\alpha^3 f_\alpha^4\hat{n}_1\left(\epsilon_{42}\right), && (4.A.30)\\
B_\alpha^6 &= -\left(f_\alpha^1\right)^2\hat{n}_1\left(\epsilon_{21}\right)-\left(f_\alpha^2\right)^2\left\{\hat{n}_1\left(\epsilon_{31}\right)+\hat{n}_2\left(\epsilon_{31}\right)\right\}-\left(f_\alpha^4\right)^2\hat{n}_1\left(\epsilon_{43}\right), && (4.A.31)\\
B_\alpha^7 &= f_\alpha^1 f_\alpha^4\left\{\hat{n}_2\left(\epsilon_{21}\right)+\hat{n}_2\left(\epsilon_{43}\right)\right\}, && (4.A.32)\\
B_\alpha^8 &= f_\alpha^2 f_\alpha^4\left\{\hat{n}_2\left(\epsilon_{31}\right)+\hat{n}_2\left(\epsilon_{43}\right)\right\}, && (4.A.33)\\
B_\alpha^9 &= f_\alpha^1 f_\alpha^3\left\{\hat{n}_1\left(\epsilon_{21}\right)+\hat{n}_1\left(\epsilon_{42}\right)\right\}, && (4.A.34)\\
B_\alpha^{10} &= f_\alpha^1 f_\alpha^4\left\{\hat{n}_1\left(\epsilon_{321}\right)+\hat{n}_1\left(\epsilon_{43}\right)\right\}, && (4.A.35)\\
B_\alpha^{11} &= -\left(f_\alpha^1\right)^2\hat{n}_2\left(\epsilon_{21}\right)-\left(f_\alpha^3\right)^2\left\{\hat{n}_1\left(\epsilon_{42}\right)+\hat{n}_2\left(\epsilon_{42}\right)\right\}-\left(f_\alpha^4\right)^2\hat{n}_2\left(\epsilon_{43}\right), && (4.A.36)\\
B_\alpha^{12} &= f_\alpha^2 f_\alpha^3\left\{\hat{n}_1\left(\epsilon_{31}\right)+\hat{n}_1\left(\epsilon_{42}\right)\right\}, && (4.A.37)\\
B_\alpha^{13} &= f_\alpha^2 f_\alpha^4\left\{\hat{n}_1\left(\epsilon_{31}\right)+\hat{n}_1\left(\epsilon_{43}\right)\right\}, && (4.A.38)\\
B_\alpha^{14} &= -\left(f_\alpha^2\right)^2\hat{n}_2\left(\epsilon_{31}\right)-\left(f_\alpha^3\right)^2\hat{n}_2\left(\epsilon_{42}\right)-\left(f_\alpha^4\right)^2\left\{\hat{n}_1\left(\epsilon_{43}\right)+\hat{n}_2\left(\epsilon_{43}\right)\right\}, && (4.A.39)
\end{aligned}
$$

$$
C_\alpha = -\left(f_\alpha^1\right)^2\hat{n}_1\left(\epsilon_{21}\right)-\left(f_\alpha^2\right)^2\hat{n}_1\left(\epsilon_{31}\right)-\left(f_\alpha^3\right)^2\hat{n}_2\left(\epsilon_{42}\right)-\left(f_\alpha^4\right)^2\hat{n}_2\left(\epsilon_{43}\right). \qquad (4.A.40)
$$

The matrices of the damping term in (4.3.24) originated from (4.3.3) are given by

$$
\boldsymbol{Q}_+^A = \begin{pmatrix} A_+^1 & 0 & 0 & 0 & 0 & A_+^2 \\ 0 & 0 & 0 & 0 & 0 & 0 \\ 0 & 0 & 0 & 0 & 0 & 0 \\ 0 & 0 & 0 & 0 & 0 & 0 \\ 0 & 0 & 0 & 0 & 0 & 0 \\ -A_+^1 & 0 & 0 & 0 & 0 & -A_+^2 \end{pmatrix}, \qquad (4.A.41)
$$

$$
\boldsymbol{Q}_+^B = \begin{pmatrix} B_+^1 & 0 & 0 & 0 \\ 0 & B_+^1 & 0 & 0 \\ 0 & 0 & B_+^2 & 0 \\ 0 & 0 & 0 & B_+^2 \end{pmatrix} \qquad (4.A.42)
$$

and

$$\boldsymbol{Q}_{+}^{C} = C_{+}, \tag{4.A.43}$$

where

$$A_{+}^{1} = -2\hat{n}_1\left(\epsilon_{41}\right), \tag{4.A.44}$$

$$A_{+}^{2} = 2\hat{n}_2\left(\epsilon_{41}\right), \tag{4.A.45}$$

$$B_{+}^{1} = -\hat{n}_1\left(\epsilon_{41}\right), \tag{4.A.46}$$

$$B_{+}^{1} = -\hat{n}_2\left(\epsilon_{41}\right), \tag{4.A.47}$$

$$C_{+} = -\hat{n}_1\left(\epsilon_{41}\right) - \hat{n}_2\left(\epsilon_{41}\right) \tag{4.A.48}$$

whereas

$$\boldsymbol{Q}_{-}^{A} = \begin{pmatrix} 0 & 0 & 0 & 0 & 0 & 0 \\ 0 & A_{-}^{1} & 0 & 0 & A_{-}^{2} & 0 \\ 0 & A_{-}^{3} & A_{-}^{4} & A_{-}^{5} & A_{-}^{6} & 0 \\ 0 & A_{-}^{3} & A_{-}^{5} & A_{-}^{4} & A_{-}^{6} & 0 \\ 0 & -A_{-}^{1} & 0 & 0 & -A_{-}^{2} & 0 \\ 0 & 0 & 0 & 0 & 0 & 0 \end{pmatrix}, \tag{4.A.49}$$

$$\boldsymbol{Q}_{-}^{B} = \begin{pmatrix} B_{-}^{1} & B_{-}^{2} & 0 & 0 \\ B_{-}^{3} & B_{-}^{4} & 0 & 0 \\ 0 & 0 & B_{-}^{1} & B_{-}^{2} \\ 0 & 0 & B_{-}^{3} & B_{-}^{4} \end{pmatrix}, \tag{4.A.50}$$

and

$$\boldsymbol{Q}_{-}^{C} = 0, \tag{4.A.51}$$

where

$$A_{-}^{1} = -2\left(\sin^4\theta + \cos^4\theta\right)\hat{n}_1\left(\epsilon_{32}\right), \tag{4.A.52}$$

$$A_{-}^{2} = 2\left(\sin^4\theta + \cos^4\theta\right)\hat{n}_2\left(\epsilon_{32}\right), \tag{4.A.53}$$

$$A_{-}^{3} = -2\cos\theta\sin\theta\left(\cos^{2}\theta-\sin^{2}\theta\right)\hat{n}_{1}\left(\epsilon_{32}\right), \tag{4.A.54}$$

$$A_{-}^{4} = -\left(\sin^{4}\theta+\cos^{4}\theta\right)\left\{\hat{n}_{1}\left(\epsilon_{32}\right)+\hat{n}_{2}\left(\epsilon_{32}\right)\right\}, \tag{4.A.55}$$

$$A_{-}^{5} = -2\sin^{2}\theta\cos^{2}\theta\left\{\hat{n}_{1}\left(\epsilon_{32}\right)+\hat{n}_{2}\left(\epsilon_{32}\right)\right\}, \tag{4.A.56}$$

$$A_{-}^{6} = 2\cos\theta\sin\theta\left(\cos^{2}\theta-\sin^{2}\theta\right)\hat{n}_{2}\left(\epsilon_{32}\right), \tag{4.A.57}$$

$$B_{-}^{1} = -\left(\sin^{4}\theta+\cos^{4}\theta\right)\hat{n}_{1}\left(\epsilon_{32}\right), \tag{4.A.58}$$

$$B_{-}^{2} = \cos\theta\sin\theta\left(\cos^{2}\theta-\sin^{2}\theta\right)\hat{n}_{2}\left(\epsilon_{32}\right), \tag{4.A.59}$$

$$B_{-}^{3} = -\cos\theta\sin\theta\left(\cos^{2}\theta-\sin^{2}\theta\right)\hat{n}_{1}\left(\epsilon_{32}\right), \tag{4.A.60}$$

$$B_{-}^{4} = -\left(\sin^{4}\theta+\cos^{4}\theta\right)\hat{n}_{2}\left(\epsilon_{32}\right). \tag{4.A.61}$$

Bibliography

[1] I. Solomon and N. Bloembergen, J. Chem. Phys. **25**, 261 (1953),
I. Solomon, Phys. Rev. **99**, 559 (1955),
N. Bloembergen, Phys. Rev. **104**, 1542 (1956).

[2] A. Abragam, *The Principle of Nuclear Magnetism*,
(Clarendon Press, Oxford, 1961).

[3] A. Barenco and A. Ekert, Acta Phys. Slovaca **45**, 205 (1995),
A. Ekert and R. Jozsa, Rev. Mod. Phys. (to appear).

[4] See for instance, W.E. Louisell, *Quantum Statistical Properties of Radiation*,
(John Wiley & Sons, Inc., New York, 1973).